Received: 12 April 2019 | Revised: 6 June 2019 | Accepted: 29 June 2019

DOI: 10.1002/er.4735

RESEARCH ARTICLE

WILEY INTERNATIONAL JOURNAL OF ENERGY RESEARCH

A correction to the unimodal and bimodal truncated normal distributions for a more accurate representation of extreme and calm wind speeds

Domenico Mazzeo | **Giuseppe Oliveti** | **Alberta Marsico**

Department of Mechanical, Energy and Management Engineering (DIMEG), University of Calabria, P. Bucci 46/C, Rende 87036, Italy

Correspondence
Domenico Mazzeo, Department of Mechanical, Energy and Management Engineering (DIMEG), University of Calabria, P. Bucci 46/C, Rende, Italy.
Email: domenico.mazzeo@unical.it

Summary

The use of wind speed probability density functions is a standard practice to represent different wind regimes. Generally, these regimes are distinguished by the following three characteristics: the shape of the distribution in the central wind speeds, amount of the calm wind speeds (CWS), and extreme wind speeds (EWS). An in-depth review has highlighted that none of the parametric distributions available is suitable to represent the three main characteristics at the same time.

To overcome this gap, the use of the corrected mixture of two truncated normal distributions (CMTTND) and corrected single truncated normal distribution (CTND) are proposed to represent, respectively, bimodal and unimodal wind speed distribution shapes. The CMTTND and CTND are obtained by introducing a correction, respectively, to the mixture of two truncated normal distributions (MTTND) and to the single truncated normal distribution (TND). The MTTND and TND permit an accurate representation of distributions with high levels of CWS. The CMTTND and CTND employ a new parameter, to accurately quantifying also the relative frequencies associated with EWS. The performance of the CMTTND and CTND was assessed using a goodness-of-fit (GOF) test and statistical measures of error in the evaluation of the characteristic mean wind speeds. The analytical expressions of these mean wind speeds are obtained and validated by a numerical integration method for the first time in this work. The accuracy of these distributions is compared with that of other conventional probability distribution models, of which three are unimodal and six bimodal, in four Italian locations and three American locations. The analysis of the results showed that the CTND and CMTTND allow obtaining high GOF of the experimental distributions with R^2 and RMSE higher and lower than, respectively, 0.977 and 0.054. Moreover, the CTND results in the most accurate distribution in the estimation of the characteristic mean wind speeds in the case of localities with unimodal experimental distributions and the CMTTND in the case of localities with bimodal experimental distributions. Contrary to other distribution, CTND and CMTTND accuracies grow by increasing the grade of the characteristic mean wind speed by reaching also estimation values lower than 2% of the real ones. This is a great advantage in

the wind energy source determination in a location since the available energy depends on the mean cubic wind speed.

KEYWORDS

Calm wind speeds, Distribution correction, Extreme wind speeds, Normal Distribution, Mixture distribution, Statistical analysis

1 | INTRODUCTION

The growth of the world population and the rapid increase in the use of fossil fuels, considered to be among the main causes of environmental pollution, have encouraged the development of clean energy sources, mainly solar and wind energy. In particular, the rapid spread of wind energy technologies has made wind energy a viable alternative to conventional energy in recent years.[1] The use of the wind resource in a location requires a detailed study of wind characteristics, and in the first phase, it is very useful to have predictive analytical models of statistical distributions able to approximate the real wind speed distributions and their main properties. Generally, three main distribution characteristics can be distinguished: the shape of the distribution in the central wind speeds, amount of the calm wind speeds (CWS), and extreme wind speeds (EWS).

1.1 | Literature review

In the following subsections, a literature overview is presented to highlight the main researches developed to describe unimodal and bimodal distributions in the central wind speeds, the main disadvantages of these distributions to models CWS and EWS, and the most important distributions proposed to overcome these issues.

1.1.1 | Single and mixture distributions

Among the mathematical models originally used, the one-parameter Rayleigh distribution and the two-parameter Weibull distributions have become the most widespread and accepted probability distributions given their simplicity.[2-7] Other distributions largely employed worldwide are the lognormal, truncated normal, gamma, inverse normal, beta, and generalized gamma distributions.[8] For example, the effectiveness of the popular Weibull and Rayleigh distributions was assessed in North Dakota (USA) by considering also other distributions such as gamma, lognormal, and inverse normal derived probability density functions (PDFs).[9] In another study, three PDFs, ie, Weibull, logistic, and lognormal, were compared to select the best one to model wind speed distribution in Inner Mongolia, China.[10]

Recently, Alavi et al studied the performance of Nakagami distribution against some previously used PDFs including exponential, Weibull, gamma, lognormal, loglogistic, inverse normal, and generalized extreme value in Iran.[11] Instead, in another study, the extended generalized Lindley distribution was proposed and evaluated to show its capability in estimating wind speed data in different regions of Turkey compared with the Weibull, Rayleigh, lognormal, and gamma distributions.[12] Similarly, Weibull, gamma, inverse normal, lognormal, Gumbel, generalized extreme value, Nakagami, and generalized logistic distribution were directly compared in Algeria.[13] Masseran proposed an integrated rank approach in determining the best model selection for wind speed data. To show the effectiveness of this method, the lognormal, Weibull, Rayleigh, exponential, Burr, gamma, inverse Gaussian, and inverse gamma distributions were considered and applied to model the wind speed regimes in Malaysia.[14]

A further variant of the Weibull distribution is the upper-truncate Weibull distribution,[15] which can be applied in situations in which the range of the random variable is bounded from above by an unknown cutoff point, called a truncation point. Other distributions used to represent wind speed data are those with three parameters of Weibull and Frechét[16] and the multiparameter distributions of Johnson, Kappa, and Wakeby.[17]

To describe the wind regimes that present bimodal trends with a double peak, several authors have proposed the use of mixtures of two distributions. In these cases, the mixture distributions are indispensable since gave rise to a better fitting of the data compared with the unimodal distributions.

Mixtures of two two-parameter Weibull distributions, of two truncated normal distributions, of a two-parameter Weibull, and a truncated normal distribution are among those mainly used. For example, Chang compared the mixture distributions gamma-Weibull and truncated normal–truncated normal, and other common distribution mixtures, such as the Weibull-Weibull and truncated

normal–Weibull, with the conventional Weibull distribution.[18]

Ouarda et al considered eleven unimodal distributions with two, three, and four parameters, and Weibull-Weibull and gamma-gamma homogeneous mixture distributions in nine stations in the United Arab Emirates (UAE) to identify the best one in terms of goodness-of-fit (GOF).[19] Subsequently, some of the previous authors represented wind speed data of Nordic regions of Canada, in addition to the two-component homogeneous distributions, also through heterogeneous (the two components are represented by two different distributions) two-component distributions.[20]

Generally, the main assumption of the different mixture distributions is that every single component is unimodal. Hu et al[21] proposed a more general model, called the hierarchical mixture of multiple distributions, in which it is assumed that each component distribution is itself a mixture. The experimental results obtained indicate that the proposed model is more accurate both for single distribution models and mixtures of single distributions. Kappa and Wakeby unimodal distributions and Burr–generalized extreme value mixture distribution were proposed by Jung et al as a single system able to reproduce a large majority of existing wind regimes around the world with very high accuracy.[22] In addition, some of these authors used the previous single and mixture distributions to evaluate the robustness of a wind speed distribution system compared with the typical deficiencies of the wind speed data, such as errors of measurement, missing data, and low temporal resolution.[23] To assess the suitability to model wind speed data in the UAE, gamma, Weibull, extreme value type I, and normal distributions were used to construct mixture distributions, while the Weibull and Kappa distributions were considered as conventional unimodal distributions.[24] Analogously to the procedure proposed by Masseran[14] that was applied only for unimodal distribution, Miao et al introduced a score-radar map to determine graphically the suitability of parametric distribution.[25] Specifically, an integrated score using different weight coefficients and typical fitting performance indices were used to test the suitability of nine well-known unimodal distributions and seven common bimodal distributions to represent wind speed data from North Dakota region.

Comprehensive reviews were carried out to analyse the flexibility and usefulness of the most common unimodal and bimodal PDFs in the description of different wind regimes (high frequencies of calm and extreme wind speeds, unimodal, bimodal, bitangential regimes, etc).[8,26] A global comparison of 24 one-component PDFs and 21 mixture PDFs in modelling onshore and offshore wind speed regimes worldwide was developed in Jung and Schindler .[27]

1.1.2 | Calm and extreme wind speeds

The statistical models described are not able to represent all the wind regimes that can occur, such as wind speed data characterized, for example, by long calm wind speeds (CWS) or high frequencies at sustained speeds (EWS). Such distributions provide a nil or undefined frequency in correspondence to a nil wind speed, whereas the trend tends asymptotically to zero for high wind speed values. Takle and Brown[28] have proposed the use of a hybrid PDF that removes the CWS and fits the non-zero wind speeds through the Weibull distribution. The CWS are then reintroduced to ensure correct values of mean and variance and to renormalize the distribution. The inverse normal distribution was suggested by Bardsley[29] as an alternative use of the three-parameter Weibull distribution, with a positive position parameter μ, for the description of the reduced wind speeds. However, it is not defined for $v = 0$ and, consequently, it cannot identify the CWS. Instead, the truncated normal distribution was used by Carta et al[30] to describe wind speed regimes with a high frequency of CWS. Also, the mixture probability distributions were used to represent wind speed data characterized by a large number of CWS. In particular, in an analysis related to the application of Weibull distribution models, Qin et al[31] proposed the use of mixtures obtained by linearly combining two two-parameter Weibull distributions, one two-parameter Weibull distribution and one three-parameter Weibull distribution and two three-parameter Weibull distributions. On the other hand, Carta and Ramìrez[32] proposed the use of a heterogeneous mixture consisting of the truncated normal distribution and the two-parameter Weibull distribution, showing that this distribution, unlike the mixture of Weibull distributions, takes into account the frequencies of the CWS.

Even more important than the correct fitting of the wind speed distributions characterized by long CWS is the correct representation of the EWS, owing to problems related to the structural safety of turbines.[33] When the wind speed is higher than the cutoff value of the turbine, the electrical generator has to be stopped to preserve the correct operation of the turbine, and the electrical energy produced is zero. Usually, this cutoff value of the turbine is close to the EWS range. In addition, the energy available in a location depends on the mean cubic wind speed, calculable as a function of the product of the relative frequencies and relative cubic wind speeds. Although if the relative frequencies of EWS are generally low, the

product of these frequencies and the extreme cubic wind speeds have relatively high values. Many of the studies relating to the theory of EWS assume that wind speed observations are independent and identically distributed variables, characterized by a common PDF: Among the most used are the Fréchet distribution, Gumbel distribution, and inverse Weibull distribution.[34] The inverse Weibull distribution is similar to the Weibull distribution, very flexible for those distributions characterized by a long asymmetric tail on the right, ie, by high frequencies at extreme wind speeds (EWS).[35] In the early 1970s, two competitive models were widely used to capture EWS data: extreme value type II distribution or Fréchet distribution and extreme value type I distribution or Gumbel distribution. In some works,[36-39] the inverse Weibull distribution was considered the best for modelling EWS when compared with the Gumbel distribution. Instead, Perrin et al[40] have shown that the inverse Weibull generates an incorrect estimate of the wind speed distribution tails and distribution of the annual wind speed maxima. According to the results obtained in these works,[36-40] neither Gumbel nor inverse Weibull distributions can be considered the best or completely adequate to model EWS. Lee et al.[41] applied the Gumbel and inverse Weibull distributions for estimating EWS in the region of Korea, demonstrating that the Gumbel distribution is much more reliable than inverse Weibull distribution. Few analyses have been carried out on how to extract the EWS reliably from a data set distributed according to the Gumbel distribution. In fact, the extraction of EWS through the Gumbel distribution strongly depends on the method used. Kang et al[42] took into account, from the wind speed time series, two types of EWS: the maximum periodic wind speeds, divided into DMWS (daily maximum wind speeds), MMWS (maximum monthly wind speeds), and YMWS (yearly maximum wind speeds), and wind speeds above a certain threshold value (top 3651, top 120, and top 10). Of the six methods used, the DMWS resulted in the best; moreover, the maximum periodic wind speeds have been better fitted by the Gumbel distribution compared with the wind speeds above a given threshold. An effective distribution, alternative to the best-known models for EWS, is the inverse Burr distribution, proposed by Chiodo and De Falco.[33] Morgan et al,[43] using the wind speed time series collected at 178 offshore stations, showed that the three-parameter Weibull, Kappa, and Wakeby distributions are the most accurate among the 11 distributions considered. In particular, the Kappa and Wakeby distributions fit better the right distribution tail, namely, the EWS, although they could drastically overestimate the relative frequencies of the lower wind speeds. For this reason, different models of mixture distributions have been proposed. The mixture distributions used for EWS estimation are two Gumbel distributions,[44] two generalized extreme value distributions,[45] two inverse Weibull distributions,[46] Gumbel–inverse Weibull mixture distributions,[47] Gumbel–generalized extreme value mixture distributions,[47] and two-component extreme value distributions.[48] A more complex model was proposed by de Waal et al,[49] which provides for the use of the multivariate generalized Burr-gamma distribution for wind speed data containing EWS. In this model, a multivariate approach is adopted, and wind speeds and directions, measured in several Dutch stations, were used to estimate the quantiles of EWS.

1.2 | Motivation and objectives of the research

Table 1 highlights the capability and limitations of the most widespread distributions used to represent wind speed with the indication of those able to represent CWS, EWS, and bimodal behaviours. Although if less frequent, three modal behaviours or above, namely, with more than two peaks, cannot be predicted very accurately by any of the distributions selected.

As regards the mixture distributions, the following criterion was adopted for the identification of the capability and the limitations in representation of CWS and EWS: The mixture distribution is able to represent EWS when both component distributions are suitable for EWS; the mixture distribution is able to represent CWS when at least one component distribution is suitable for CWS and the other one must be at least defined.

From the analysis of all the distributions reported in Table 1, it is evident the lack of a flexible distribution of general use able to represent all wind speed regimes.

This paper proposes the use of the corrected mixture of two truncated normal distributions (CMTTND) with six parameters, of which five are independent, to statistically represent the measured wind speed data. The truncation of the normal distributions is necessary to eliminate the negative wind speeds while the correction made allows improving the representation of the EWS. This model is capable to represent unimodal and bimodal distributions, characterized by CWS and EWS.

The single-corrected truncated normal distribution (CTND), with one dependent and two independent parameters, provides a correction to the truncated normal distribution (TND), already used by several researchers for the representation of wind speed data.[18,50-52]

From the scientific literature, the TND can be obtained from the ND with two different approaches.

TABLE 1 Literature survey of the statistical distribution for the representation of the CWS and EWS and bimodal behaviour

Distributions	Number of Parameters	Calm Wind Speeds	Extreme Wind Speeds	Bimodal Shape
Unimodal distributions				
Rayleigh	1	No	No	No
Exponential	1	Yes	No	No
Two-parameter Weibull (extreme value type III)	2	No	No	No
Generalized Rayleigh	2	No	No	No
Two-parameter lognormal	2	No	No	No
Normal	2	Yes	No	No
Gamma	2	No	No	No
Beta	2	No	Yes	No
Logistic	2	Yes	No	No
Loglogistic	2	No	No	No
Truncated normal	2	Yes	No	No
Upper-truncate Weibull	2	No	Yes	No
Nakagami	2	No	No	No
Inverse normal	2	No	No	No
Gumbel (extreme value type I)	2	No	Yes	No
Frechet or inverse Weibull (extreme value type II)	2	No	Yes	No
Three-parameter lognormal	3	Yes	No	No
Burr	3	No	No	No
Three-parameter Weibull	3	Yes	No	No
Log Pearson type III	3	No	Yes	No
Generalized logistic	3	Yes	No	No
Generalized gamma (Pearson type III)	3	No	No	No
Generalized extreme value	3	No	Yes	No
Dagum (inverse Burr)	3	No	Yes	No
Extended generalized Lindley	3	Yes	No	No
Kappa	4	Yes	Yes	No
Johnson	4	No	No	Yes
Wakeby	5	Yes	Yes	No
Homogeneous bimodal distributions				
Mixture of two normal	5	Yes	No	Yes
Mixture of two-parameter Weibull	5	No	No	Yes
Mixture of two Gumbel	5	No	Yes	Yes
Mixture of two inverse Weibull	5	No	Yes	Yes
Mixture of two gamma	5	No	No	Yes
Mixture of two three-parameter Weibull	7	Yes	No	Yes
Mixture of two generalized extreme value	7	No	Yes	Yes
Heterogeneous bimodal distributions				
Mixture of a two-parameter Weibull and a truncated normal	5	Yes	No	Yes
Mixture of a Gumbel and an inverse Weibull	5	No	Yes	Yes

(Continues)

TABLE 1 (Continued)

Distributions	Number of Parameters	Calm Wind Speeds	Extreme Wind Speeds	Bimodal Shape
Mixture of a gamma and a Weibull	5	No	No	Yes
Mixture of a gamma and a Gumbel	5	No	No	Yes
Mixture of a Weibull and a Gumbel	5	No	No	Yes
Mixture of a normal and a Weibull	5	Yes	No	Yes
Mixture of a normal and a Gumbel	5	Yes	No	Yes
Mixture of a normal and a Gamma	5	No	No	Yes
Mixture of two truncated normal	5	Yes	No	Yes
Mixture of a two-parameter Weibull and a three-parameter Weibull	6	Yes	No	Yes
Mixture of a Gumbel and a generalized extreme value	6	No	Yes	Yes
Multivariate generalized Burr-gamma	6	No	Yes	Yes
Mixture of a Weibull and a Burr	6	No	No	Yes
Mixture of a truncated normal and a Burr	6	Yes	No	Yes
Mixture of a Burr and a generalized extreme value	7	No	No	Yes
Mixture of two Burr	7	No	No	Yes
Corrected truncated normal	**3**	**Yes**	**Yes**	**No**
Corrected mixture of two truncated normal	**6**	**Yes**	**Yes**	**Yes**

The Corrected truncated normal and Corrected mixture of two truncated normal are the two Distributions proposed in this work.

The most used approach foresees to annul the ND for $v < 0$ and to divide it by the area subtended by the ND for $v > 0$. This means that the truncated area for $v < 0$ is spread in a relatively uniform manner in the domain $0 \le v < +\infty$ without using a physical criterion[18,50,51]; see Equation (1). In this way, the area truncated is recovered, and a unitary value of area subtended by the TND is obtained.

$$f_{\mathrm{TND}}(v) = \begin{cases} 0 & v < 0 \\ \dfrac{\dfrac{1}{\sigma\sqrt{2\pi}}\exp\left[-\dfrac{1}{2}\left(\dfrac{v-\mu}{\sigma}\right)^2\right]}{\dfrac{1}{2}\left[1 + \mathrm{erf}\left(\dfrac{\mu}{\sqrt{2}\sigma}\right)\right]} & v \ge 0 \end{cases} \quad (1)$$

Instead, in other researches,[52] a piecewise function was used, Equation (2), in which the truncated area for $v < 0$ was not spread in the domain $0 \le v < +\infty$ as in Equation (1).

$$f_{\mathrm{TND}}(v) = \begin{cases} 0 & v < 0 \\ \dfrac{1}{\sigma\sqrt{2\pi}}\exp\left[-\dfrac{1}{2}\left(\dfrac{v-\mu}{\sigma}\right)^2\right] & v \ge 0 \end{cases} \quad (2)$$

This approach presents the advantage of making the determination procedure of the distribution parameters simpler and computationally less expensive. However, despite this approach leads to a correct representation of the wind speeds that are zero or near zero, it does not respect the constraint of the unitary value of the area subtended to the distribution. Definitively, this approach is very accurate only when the area subtended for $v < 0$ is small.

Summarizing, on the one hand, the truncation leads to a correct representation of the statistical distribution characterized by high frequencies at reduced wind speeds, but on the other hand,

- When the approach of Equation (1) is used, namely, the area subtended for $v < 0$ is spread in the entire domain $0 \le v < +\infty$, all relative frequencies indiscriminately increases;
- When the approach of Equation (2) is used, namely, the area subtended for $v < 0$ is not spread in the entire domain $0 \le v < +\infty$, the relative frequencies corresponding to the high wind speeds, namely, the EWS, are usually underestimated.[52]

An incorrect interpolation of the relative frequencies of the EWS gives rise to an underestimation of the mean, mean square, and mean cubic wind speeds. Specifically, the calculation of the characteristic mean wind speeds, respectively, is determined by the products, between v and $f(v)$, v^2, and $f(v)$, and v^3 and $f(v)$. Therefore, the underestimation of the relative frequencies of the EWS determines a more accentuated error by increasing the

grade of the mean wind speed. This is important since the available average power and energy are directly proportional to the mean cubic wind speed, while some important wind properties, such as the standard deviation and Fisher asymmetry, are dependent on the mean and mean square wind speeds, as described in the successive section.

In a very similar way, the problems related to the truncation of the ND can be extended to the mixture of two truncated normal distributions (MTTND). This distribution, in addition to allowing the problem of the correct representation of the CWS to be overcome, allows reproducing bimodal trends. However, also, this distribution is usually not able to describe distributions characterized by frequent EWS.[52]

The main objective of this paper is to propose a correction to the two-parameter TND and five-parameter MTTND for a more accurate representation of unimodal or bimodal shapes at the centre wind speeds, CWS, and EWS simultaneously. Starting from the approach of Equation (2), the CTND and CMTTND proposed permit to recovery with a physical criterion the area lost in the truncation process for $v < 0$ to improve the overall accuracy. This criterion consists of spreading the truncated area only in proximity to the EWS values. In particular, a corrective function dependent on a new parameter characterizing the EWS was introduced. For the first time, analytical expressions of the characteristic mean wind speeds of these distributions were obtained and validated using the numerical integration method.

The CTND and CMTTND accuracies were compared with that of the most common unimodal and bimodal distributions by using different GOF test and by calculating the box plots of errors in the determination of the characteristic mean wind speeds in some Italian and American meteorological stations.[53,54]

2 | METHODOLOGY

2.1 | Characterization of the wind speed data

The availability of the wind resource is modelled by means of analytical functions able to approximate the statistical distributions of real wind speed intensity data over a long period and some relevant properties (mean wind speed, extreme wind speeds, irregularities, and so on). Having a sample of mean wind speed data calculated considering a time interval Δt, for example, of 10 minutes, concerning an observation period T equal to one or more years, it is possible to calculate the mean wind speed, mean square wind speed, and mean cubic wind speed, characteristics of the entire observation period, Equations (3a), (3b), and (3c):

$$V_{m1} = \frac{1}{N}\sum_{i=1}^{N} V_i \tag{3a}$$

$$V_{m2} = \left(\frac{1}{N}\sum_{i=1}^{N} V_i^2\right)^{1/2} \tag{3b}$$

$$V_{m3} = \left(\frac{1}{N}\sum_{i=1}^{N} V_i^3\right)^{1/3} \tag{3c}$$

where

V_i is the ith experimental mean wind speed related to the time interval $\Delta t = T/N$, with N the number of wind speed observations;

V_{m1}, V_{m2}, and V_{m3} are the characteristic mean wind speeds in the entire observation period T.

The characteristic mean wind speeds are very useful to evaluate important wind properties of a locality.

The mean cubic wind speed allows calculation of the available mean power P_a, Equation (4), and the available energy E_a, Equation (5):

$$P_a = \frac{1}{2}\rho A_0 V_{m3}^3, \tag{4}$$

$$E_a = P_a T = \frac{1}{2}\rho A_0 V_{m3}^3 T, \tag{5}$$

where

ρ is the air density and

A_0 is the swept area of blades.

The mean and mean square wind speeds are used to quantify the standard deviation σ, namely, the dispersion of the wind speed values compared to the mean value:

$$\sigma = \left[\frac{\sum_{i=1}^{N}[V_i - V_{m1}]^2}{N}\right]^{1/2} = \left(V_{m2}^2 - V_{m1}^2\right)^{1/2}. \tag{6}$$

The discrete PDF $f(V_i)$ is used to statistically represent a sufficiently large sample of wind speed. The asymmetry of this distribution is quantifiable by the Fisher coefficient γ, Equation (7), the ratio of the central moment of the third order, and the cube of the standard deviation. This coefficient can be easily calculable starting from the use of all the characteristic mean wind speeds:

$$\gamma = \frac{\frac{\sum_{i=1}^{N}(V_i - V_{m1})^3}{N}}{\sigma^3} = \frac{V_{m3}^3 - 3V_{m2}^2 V_{m1} + 2V_{m1}^2}{\sigma^3}. \tag{7}$$

The discrete PDF can be described analytically by the continuous PDF $f(v)$, which has the fundamental property of the unitary subtended area. Starting from $f(v)$, it is possible to calculate the relative frequency of all the

wind speeds that are lower than a given value v, to obtain in this way, the cumulative density function (CDF) $F(v)$, expressed by Equation (8):

$$F(v) = \int_0^v f(\xi)d\xi. \tag{8}$$

The general analytical expressions for the calculation of the characteristic mean wind speeds as a function of $f(v)$ are expressed by Equations (9a), (9b), and (9c).

$$V_{m1} = \frac{\int_0^{+\infty} v f(v)dv}{\int_0^{+\infty} f(v)dv} \tag{9a}$$

$$V_{m2} = \left(\frac{\int_0^{+\infty} v^2 f(v)dv}{\int_0^{+\infty} f(v)dv}\right)^{1/2} \tag{9b}$$

$$V_{m3} = \left(\frac{\int_0^{+\infty} v^3 f(v)dv}{\int_0^{+\infty} f(v)dv}\right)^{1/3} \tag{9c}$$

For some continuous distributions, it is possible to solve analytically the integrals of the Equations (9a), (9b), and (9c). In other cases, when $f(v)$ has a complex analytical structure, numerical integration is used.

2.2 | Correction of the unimodal and bimodal truncated normal distributions

2.2.1 | Corrected truncated normal distribution (CTND)

PDF and CDF

The PDF of the CTND, $f_{CTND}(v)$, was defined starting from the TND, $f_{TND}(v)$, in turn obtained from an ND by eliminating all relative frequencies for $v < 0$. In particular, to restore the unit value of the area subtended by the distribution, the truncated area was used to increase the relative frequencies of only the EWS. The PDF of the CTND is a piecewise function defined by Equation (10):

$$f_{CTND}(v) = \begin{cases} 0 & v < 0 \\ \frac{1}{\sigma\sqrt{2\pi}} \exp\left[-\frac{1}{2}\left(\frac{v-\mu}{\sigma}\right)^2\right] & 0 \le v < \mu + \sigma \\ \frac{1}{\sigma\sqrt{2\pi}} \exp\left[-\frac{1}{2}\left(\frac{v-\mu}{\sigma}\right)^2\right] + g(v) & v \ge \mu + \sigma \end{cases} \tag{10}$$

where μ is the position parameter of the TND, ie, the mean, σ is the shape parameter of the TND, ie, the standard deviation, and $g(v)$ is a corrective function of the EWS.

The subdomain of EWS was identified starting from the second inflexion of the TND, ie, from the wind speed $v = \mu + \sigma$, in which the tangent to the TND reaches the minimum value and the concavity is inverted. The function $g(v)$ must respect the following constraints:

1) $g(v)$ has a positive domain ($v \ge 0$), since the wind speed can only assume values greater than or zero, and positive codomain ($g(v) \ge 0$), since the function $g(v)$ has the task to increase the relative frequencies starting from the inflexion point $v = \mu + \sigma$;
2) to make the area subtended by the CTND unitary, the area between the function $f_{TND}(v)+g(v)$ and the function $f_{TND}(v)$, for $v > \mu + \sigma$, must be equal to the area removed as a result of the truncation;
3) the continuity condition requires a value of the function $g(\mu + \sigma) = 0$ in the point $v = \mu + \sigma$;
4) the function $g(v)$ must tend to zero for v tending to $+\infty$ and, taking into account condition 3), the function $g(v)$ must have a maximum.

The function $g(v)$ that satisfies conditions 1), 3), and 4) can be placed in the following form:

$$g(v) = [v - (\mu + \sigma)] \exp\left(-\frac{v}{K_I}\right). \tag{11}$$

The new parameter K_I, characteristic of the CTND, is the extreme wind speed parameter, index of the entity of the relative frequencies of the EWS.

Replacing Equation (10) into Equation (8) and by solving the integral, the CDF equation is obtained, Equation (12).

$$F_{CTND}(v) = \begin{cases} 0 & v < 0 \\ \frac{1}{2}\left[1 + \text{erf}\left(\frac{v-\mu}{\sqrt{2}\sigma}\right)\right] & 0 \le v < \mu + \sigma \\ \frac{1}{2}\left[1 + \text{erf}\left(\frac{v-\mu}{\sqrt{2}\sigma}\right)\right] - K_I \exp\left(-\frac{v}{K_I}\right)(K_I - \mu - \sigma + v) + K_I^2 \exp\left(-\frac{\mu+\sigma}{K_I}\right) & v \ge \mu + \sigma \end{cases} \tag{12}$$

Determination of the parameter K_I

The analytical expression of the parameter K_I is obtained from condition 2) of the PDF and CDF section:

$$\int_{\mu+\sigma}^{+\infty} g(v)dv = (1 - A_I), \tag{13}$$

where A_I is the area subtended by the TND, complement to one of the CDF $F_{CTND}(v)$ for $v = 0$.

$$(1 - A_I) = F_{CTND}(0) = \frac{1}{2}\left[1 - \text{erf}\left(\frac{\mu}{\sqrt{2}\sigma}\right)\right] \tag{14}$$

The resolution of the integral in Equation (13) leads to the equality $K_I^2 \exp[-(\mu + \sigma)/K_I] = (1 - A_I)$. This equation has two solution roots, of which only the positive one allows respecting constraint 4), Equation (15).

$$K_I = \frac{(\mu+\sigma)/2}{\text{lambertw}\left(0,\ \frac{(\mu+\sigma)}{2}\cdot\left\{\frac{1}{2}\left[1-\text{erf}\left(\frac{\mu}{\sqrt{2}\sigma}\right)\right]\right\}^{-1/2}\right)}, \tag{15}$$

where lambertw(0,x) is the principal branch of the Lambert W function. The Lambert W function $W(x)$ is a set of solutions of the equation $x = W(x)e^{W(x)}$.

The parameter K_I is determined by the two parameters μ and σ of the TND. Consequently, the correction made by means of the function $g(v)$ does not increase the computational burden of the calculation compared with that of the TND, since K_I is a dependent parameter that can be calculated explicitly once the TND parameters are known.

Characteristic mean wind speeds of the CTND

The piecewise function that defines the CTND, Equation (10), was used to determine the mathematical expressions of the characteristic mean wind speeds, taking into account that the area subtended by the CTND is unitary, $\int_0^{+\infty} f_{CTND}(v)dv = 1$.

- Mean wind speed

The mean wind speed of the CTND $V_{m1,CTND}$ can be calculated as a function of the mean wind speed of the TND $V_{m1,TND}$,[52] as demonstrated by Equations (16) and (17).

$$\begin{aligned} V_{m1,CTND} &= \frac{\int_0^{+\infty} v\, f_{CTND}(v)dv}{\int_0^{+\infty} f_{CTND}(v)dv} = \int_0^{+\infty} v\, f_{CTND}(v)dv \\ &= \int_0^{+\infty} v\, f_{TND}(v)dv + \int_{\mu+\sigma}^{+\infty} v\, g(v)dv, \end{aligned} \tag{16}$$

$$\begin{aligned} V_{m1,CTND} &= \frac{\int_0^{+\infty} v\, f_{TND}(v)dv}{\int_0^{+\infty} f_{TND}(v)dv}\int_0^{+\infty} f_{TND}(v)dv \\ &+ \int_{\mu+\sigma}^{+\infty} v\, g(v)dv = V_{m,TND}\, A_I \\ &+ \int_{\mu+\sigma}^{+\infty} v\, g(v)dv = V_{m1,TND}\, A_I \\ &+ \Delta V_{m1,CTND}, \end{aligned} \tag{17}$$

where $V_{m1,TND}$ is expressed by the equation reported in the Appendix, A_I is the area subtended by the TND, and $\Delta V_{m1,CTND}$ is the mean wind speed correction that is expressed by Equation (18).

$$\begin{aligned} \Delta V_{m1,CTND} &= \int_{\mu+\sigma}^{+\infty} v\, g(v)dv \\ &= K_I^2(\mu + \sigma + 2K_I)\ \exp\left(-\frac{(\mu+\sigma)}{K_I}\right). \end{aligned} \tag{18}$$

- Mean square wind speed

The mean square wind speed of the CTND $V_{m2,CTND}$ can be calculated as a function of the mean square wind speed of the TND $V_{m2,CTND}$,[52] as demonstrated by Equations (19) and (20).

$$\begin{aligned} V_{m2,CTND}^2 &= \frac{\int_0^{+\infty} v^2 f_{CTND}(v)dv}{\int_0^{+\infty} f_{CTND}(v)dv} \\ &= \int_0^{+\infty} v^2 f_{TND}(v)dv + \int_{\mu+\sigma}^{+\infty} v^2\, g(v)dv, \end{aligned} \tag{19}$$

$$\begin{aligned} V_{m2,CTND}^2 &= \frac{\int_0^{+\infty} v^2 f_{TND}(v)dv}{\int_0^{+\infty} f_{TND}(v)dv}\int_0^{+\infty} f_{TND}(v)dv \\ &+ \int_{\mu+\sigma}^{+\infty} v^2\, g(v)dv \\ &= V_{m2,TND}^2\, A_I \quad + \int_{\mu+\sigma}^{+\infty} v^2\, g(v)dv \\ &= V_{m2,TND}^2\, A_I \quad + \Delta V_{m2,CTND}^2, \end{aligned} \tag{20}$$

where $V_{m2,TND}^2$ is expressed by the equation reported in the Appendix and $\Delta V_{m2,CTND}^2$ is the mean square wind speed correction that is expressed by Equation (21).

$$\begin{aligned} \Delta V_{m2,CTND}^2 &= K_I^2\left[(\mu+\sigma)^2 + 4K_I(\mu+\sigma) + 6K_I^2\right] \\ &\exp\left(-\frac{(\mu+\sigma)}{K_I}\right). \end{aligned} \tag{21}$$

- Mean cubic wind speed

The mean cubic wind speed of the CTND $V_{m3,CTND}$ can be calculated as a function of the mean cubic wind speed of the TND $V_{m3,CTND}$,[52] as demonstrated by Equations (22) and (23).

$$V^3_{\mathrm{m3,CTND}} = \frac{\int_0^{+\infty} v^3 f_{\mathrm{CTND}}(v)dv}{\int_0^{+\infty} f_{\mathrm{CTND}}(v)dv} = \int_0^{+\infty} v^3 f_{\mathrm{TND}}(v)dv + \int_{\mu+\sigma}^{+\infty} v^3\, g(v)dv, \quad (22)$$

$$V^3_{\mathrm{m3,CTND}} = \frac{\int_0^{+\infty} v^3 f_{\mathrm{TND}}(v)dv}{\int_0^{+\infty} f_{\mathrm{TND}}(v)dv}\int_0^{+\infty} f_{\mathrm{TND}}(v)dv + \int_{\mu+\sigma}^{+\infty} v^3\, g(v)dv = V^3_{\mathrm{m3,TND}}\, A_{\mathrm{I}} \quad + \int_{\mu+\sigma}^{+\infty} v^3\, g(v)dv = V^3_{\mathrm{m3,TND}}\, A_{\mathrm{I}} + \Delta V^3_{\mathrm{m3,CTND}}, \quad (23)$$

where $V^3_{\mathrm{m3,TND}}$ is expressed by the equation reported in the Appendix and $\Delta V^3_{\mathrm{m3,CTND}}$ is the mean cubic wind speed correction that is expressed by Equation (24).

$$\Delta V^3_{\mathrm{m3,CTND}} = K_{\mathrm{I}}^2\left[(\mu+\sigma)^3 + 6K_{\mathrm{I}}(\mu+\sigma)^2 + 18K_{\mathrm{I}}^2(\mu+\sigma) + 24K_{\mathrm{I}}^3\right] \times \exp\left(-\frac{(\mu+\sigma)}{K_{\mathrm{I}}}\right). \quad (24)$$

Equations (17), (20), and (23) show that a given characteristic mean wind speed of CTND depends on the corresponding characteristic mean wind speed of the TND, area subtended by the TND, and on the relative mean wind speed correction, in turn dependent on the parameter K_{I}. All these quantities are only determined by the mean μ and standard deviation σ of the TND.

2.2.2 | Corrected mixture of two truncated normal distributions (CMTTND)

PDF and CDF

The PDF of the proposed CMTTND in this work was defined starting from the PDF of the MTTND,[52] a mixture of two TNDs, respectively, with mean μ_1 and μ_2, variance σ_1 and σ_2, and weight w_1 and w_2. The condition of the unitary area subtended by the distribution in the domain $(-\infty, +\infty)$ for the MTTND leads to the equation $w_1+w_2 = 1$.

The correction to be made to the MTTND to take into account the truncated area is similar to that already described in Section 2.2.1. Unlike the CTND, whose correction has been made starting from the inflexion point $v = \mu + \sigma$ of the TND, in the mixture distribution, it is necessary to establish on which of the two TNDs to make the correction. Based on the results of the study presented in Mazzeo et al,[52] it is possible to attribute the underestimation of relative frequencies related to the high wind speeds to the TND with μ_2 greater than μ_1, ie, the TND closest to the EWS. Therefore, a function $h(v)$ was defined to be added to the MTTND starting from the inflexion point $v = \mu_2+\sigma_2$.

The selected function $h(v)$ must respect the same constraints and has the same characteristics as the function $g(v)$ used to define the CTND in the PDF and CDF section. The analytical expression of the three-parameter function $h(v)$ is obtained by substituting μ_2 and σ_2 to μ and σ in Equation (11). The third parameter K_{II} is the extreme wind speed parameter of the CMTTND.

The PDF of the CMTTND is a piecewise function represented by Equation (25):

$$f_{\mathrm{CMTTND}}(v) = \begin{cases} 0 & v < 0 \\ w_1\frac{1}{\sigma_1\sqrt{2\pi}}\exp\left[-\frac{1}{2}\left(\frac{v-\mu_1}{\sigma_1}\right)^2\right] + w_2\frac{1}{\sigma_2\sqrt{2\pi}}\exp\left[-\frac{1}{2}\left(\frac{v-\mu_2}{\sigma_2}\right)^2\right] & 0 \le v < \mu_2+\sigma_2 \\ w_1\frac{1}{\sigma_1\sqrt{2\pi}}\exp\left[-\frac{1}{2}\left(\frac{v-\mu_1}{\sigma_1}\right)^2\right] + w_2\frac{1}{\sigma_2\sqrt{2\pi}}\exp\left[-\frac{1}{2}\left(\frac{v-\mu_2}{\sigma_2}\right)^2\right] + (v-\mu_2-\sigma_2)\exp\left(-\frac{v}{K_{\mathrm{II}}}\right) & v \ge \mu_2+\sigma_2 \end{cases} \quad (25)$$

The CDF of the CMTTND is

$$F_{\mathrm{CMTTND}}(v) = \begin{cases} 0 & v < 0 \\ \frac{1}{2}w_1\left[1+\mathrm{erf}\left[\frac{v-\mu_1}{\sqrt{2}\sigma_1}\right]\right] + \frac{1}{2}w_2\left[1+\mathrm{erf}\left[\frac{v-\mu_2}{\sqrt{2}\sigma_2}\right]\right] - \frac{1}{2}w_1\left[1+\mathrm{erf}\left[\frac{\mu_1}{\sqrt{2}\sigma_1}\right]\right] - \frac{1}{2}w_2\left[1+\mathrm{erf}\left[\frac{\mu_2}{\sqrt{2}\sigma_2}\right]\right] & 0 \le v < \mu_2+\sigma_2 \\ \frac{1}{2}w_1\left[1+\mathrm{erf}\left[\frac{v-\mu_1}{\sqrt{2}\sigma_1}\right]\right] + \frac{1}{2}w_2\left[1+\mathrm{erf}\left[\frac{v-\mu_2}{\sqrt{2}\sigma_2}\right]\right] - \frac{1}{2}w_1\left[1+\mathrm{erf}\left[\frac{\mu_1}{\sqrt{2}\sigma_1}\right]\right] - \frac{1}{2}w_2\left[1+\mathrm{erf}\left[\frac{\mu_2}{\sqrt{2}\sigma_2}\right]\right] & \\ -K_{\mathrm{II}}\exp\left\{-\frac{v}{K_{\mathrm{II}}}\right)\{K_{\mathrm{II}}-\mu_2-\sigma_2+v) + K_{\mathrm{II}}^2\exp\left\{-\frac{\mu_2+\sigma_2}{K_{\mathrm{II}}}\right) & v \ge \mu_2+\sigma_2 \end{cases} \quad (26)$$

Determination of the parameter K_{II}

Similarly to the procedure used for the parameter K_I of the CTND, the analytical expression for the evaluation of the parameter K_{II} was obtained by imposing the condition that the area between the function $f_{MTTND}(v)+h(v)$ and the function $f_{MTTND}(v)$ is equal to the truncated area for $v < 0$.

$$\int_{\mu_2+\sigma_2}^{+\infty} h(v)dv = (1 - A_{II}), \tag{27}$$

where A_{II} is the area subtended by the MTTND, complement to one of the CDF $F_{MTTND}(v)$ for $v = 0$.

$$\begin{aligned}(1 - A_{II}) &= F_{MTTND}(0) \\ &= w_1 F_{TND,1}(0) + w_2 F_{TND,2}(0) \\ &= \left\{\frac{1}{2}w_1\left[1 - \text{erf}\left(\frac{\mu_1}{\sqrt{2}\sigma_1}\right)\right] + \frac{1}{2}w_2\left[1 - \text{erf}\left(\frac{\mu_2}{\sqrt{2}\sigma_2}\right)\right]\right\}\end{aligned} \tag{28}$$

The resolution of the integral in Equation (27) leads to the equation $K_{II}^2 \exp[-(\mu_2 + \sigma_2)/K_{II}] = (1 - A_{II})$. In an analogous manner to the CTND, this equation has two solution roots, of which only the positive one satisfies the constraint 4), Equation (29).

$$K_{II} = \frac{(\mu_2 + \sigma_2)/2}{\text{lambertw}\left(0,\ \frac{(\mu_2 + \sigma_2)}{2} \cdot \left\{\frac{1}{2}w_1\left[1 - \text{erf}\left(\frac{\mu_1}{\sqrt{2}\sigma_1}\right)\right] + \frac{1}{2}w_2\left[1 - \text{erf}\left(\frac{\mu_2}{\sqrt{2}\sigma_2}\right)\right]\right\}^{-1/2}\right)}. \tag{29}$$

The parameter K_{II} depends on the weight w_1, means μ_1 and μ_2, and variances σ_1 and σ_2 of the two TNDs. Consequently, also in this case, the correction by means of the function $h(v)$ does not increase the computational burden of the calculation compared to that of the MTTND.

Characteristic mean wind speeds of the CMTTND

Also for the CMTTND, the analytical expressions for the calculation of the mean, mean square, and mean cubic wind speeds $V_{m1,CMTTND}$, $V_{m2,CMTTND}$, and $V_{m3,CMTTND}$ were determined. The expressions obtained are analogous to Equations (17), (20), and (23) with

- the area subtended by the MTTND A_{II} to be replaced to A_I;
- the characteristic mean wind speeds of the MTTND $V_{m1,MTTND}$, $V_{m2,MTTND}$, and $V_{m3,MTTND}$ to be replaced to those related to the TND;
- the mean wind speed corrections $\Delta V_{m1,CMTTND}$, $\Delta V_{m2,CMTTND}$, and $\Delta V_{m3,CMTTND}$ calculable with Equations (18), (21), and (24) in which K_{II}, μ_2, and σ_2 are to be replaced to K_I, μ, and σ.

2.2.3 | Examples of CTNDs and CMTTNDs by varying the characteristic parameters

In this section, a systematic parametric investigation was carried out as a function of main characteristic parameters of CTND and CMTTND to show their capabilities in the statistical representation of different wind speed regimes. In particular, starting from some TNDs obtained for different values of the two parameters μ and σ, the relative CTNDs were assessed by calculating the relative values of K_I. In a similar way, starting from the same TNDs, different MTTNDs were obtained for different values of w_2, μ_2, and σ_2, and the relative values of K_{II} were evaluated to build the corresponding CMTTNDs. Table 2 lists the set of characteristic parameters employed for this parametric analysis, with the obtained values of A_I and K_I for the CTND and A_{II} and K_{II} for the CMTTND.

In particular, four different groups of CMTTNDs were considered. Each group, composed of five CMTTNDs, is related to a constant value of the parameters w_1, μ_1, σ_1, and $w_2 = (1 - w_1)$ and to different values of μ_2 and σ_2. More in detail, the variation of μ_2 and σ_2 was set in such a way that the sum $(\mu_2 + \sigma_2)$ remains constant while the ratio (μ_2/σ_2) changes. Starting from the group 1 of CMTTNDs, group 2 was obtained by exchanging only weights w_1 and w_2, group 3 was obtained by modifying only the ratio (μ_1/σ_1), and group 4 was obtained starting from group 3 by changing only $(\mu_2 + \sigma_2)$ and (μ_2/σ_2).

With reference to the CTND, Table 2 highlights that the extreme wind speed parameter K_I becomes greater by increasing the truncated area $(1 - A_I)$, obtained with a reduction of (μ/σ) and growth of $(\mu + \sigma)$.

As regards the MTTND,

- for a specific group, namely, by varying only the value of (μ_2/σ_2), the parameters K_{II} and $(1 - A_{II})$ increase by reducing (μ_2/σ_2);

TABLE 2 Characteristic parameters of some CTNDs and CMTTNDs

TND	CTND	μ	σ	$\mu+\sigma$	μ/σ	A_I	K_I				
1	1	1.00	1.00	2.00	1.00	0.84	1.041				
2	2	1.00	1.00	2.00	1.00	0.84	1.041				
3	3	1.00	1.50	2.50	0.67	0.75	1.307				
4	4	1.00	1.50	2.50	0.67	0.75	1.307				
TND	**CMTTND**	w_1	μ_1	σ_1	μ_1/σ_1	w_2	μ_2	σ_2	$\mu_2+\sigma_2$	μ_2/σ_2	A_{II}	K_{II}
1	1	0.70	1.00	1.00	1.00	0.30	1.25	1.50	2.75	0.83	0.828	1.248
	2	0.70	1.00	1.00	1.00	0.30	1.50	1.25	2.75	1.20	0.854	1.200
	3	0.70	1.00	1.00	1.00	0.30	1.75	1.00	2.75	1.75	0.877	1.154
	4	0.70	1.00	1.00	1.00	0.30	2.00	0.75	2.75	2.67	0.888	1.131
	5	0.70	1.00	1.00	1.00	0.30	2.25	0.50	2.75	4.50	0.889	1.128
2	6	0.30	1.00	1.00	1.00	0.70	1.25	1.50	2.75	0.83	0.811	1.277
	7	0.30	1.00	1.00	1.00	0.70	1.50	1.25	2.75	1.20	0.872	1.165
	8	0.30	1.00	1.00	1.00	0.70	1.75	1.00	2.75	1.75	0.924	1.036
	9	0.30	1.00	1.00	1.00	0.70	2.00	0.75	2.75	2.67	0.950	0.951
	10	0.30	1.00	1.00	1.00	0.70	2.25	0.50	2.75	4.50	0.952	0.941
3	11	0.70	1.00	1.50	0.67	0.30	1.25	1.50	2.75	0.83	0.763	1.350
	12	0.70	1.00	1.50	0.67	0.30	1.50	1.25	2.75	1.20	0.789	1.312
	13	0.70	1.00	1.50	0.67	0.30	1.75	1.00	2.75	1.75	0.811	1.276
	14	0.70	1.00	1.50	0.67	0.30	2.00	0.75	2.75	2.67	0.822	1.258
	15	0.70	1.00	1.50	0.67	0.30	2.25	0.50	2.75	4.50	0.823	1.256
4	16	0.70	1.00	1.50	0.67	0.30	4.50	1.75	6.25	2.57	0.822	2.006
	17	0.70	1.00	1.50	0.67	0.30	4.75	1.50	6.25	3.17	0.823	2.003
	18	0.70	1.00	1.50	0.67	0.30	5.00	1.25	6.25	4.00	0.823	2.002
	19	0.70	1.00	1.50	0.67	0.30	5.25	1.00	6.25	5.25	0.823	2.002
	20	0.70	1.00	1.50	0.67	0.30	5.50	0.75	6.25	7.33	0.823	2.002

- by comparing group 2 with group 1, namely, by reducing the weight w_1, the parameters K_{II} and $(1 - A_{II})$ increase for $(\mu_2/\sigma_2) < 1$ and reduce for $(\mu_2/\sigma_2) > 1$;
- by comparing group 3 with group 1, namely, by reducing the ratio (μ_1/σ_1), the parameters K_{II} and $(1 - A_{II})$ increase for any value of (μ_2/σ_2);
- by comparing group 3 with group 4, namely, by increasing the sum $(\mu_2 + \sigma_2)$ and the ratio (μ_2/σ_2) simultaneously, the truncated area $(1 - A_{II})$ is reduced while K_{II} is increased. In addition, for group 4, namely, for a high value of $(\mu_2 + \sigma_2)$, the variation of $(1 - A_{II})$ and K_{II} by varying (μ_2/σ_2) is very contained.

In this way, a width representative sample of wind speed regimes with different unimodal and bimodal behaviours and different CWS and EWS values were obtained. Figure 1 reports the functions $g(v)$ and $h(v)$ employed to correct the relative TNDs and MTTNDs on the left, the TND and the relative CTND at the centre, and the five MTTNDs and the relative CMTTNDs on the right. The different considered groups are reported in the figure from the top towards the bottom.

Definitively, the extreme wind speed parameters K_I and K_{II} quantify the extreme wind speed values and the relative frequencies at the EWS.

2.3 | Unimodal and bimodal conventional distributions

Nine conventional PDFs were considered to be compared in terms of accuracy with the CTND and the CMTTND. Three of these conventional PDFs are unimodal and six bimodal, which are obtained starting from the same unimodal distributions:

- unimodal distributions
- two-parameter Weibull distribution (W2D)
- two-parameter truncated normal distribution (TND)
- three-parameter Burr distribution (B3D)
- bimodal distributions
- mixture Weibull-Weibull distribution (W2W2D)
- mixture Weibull–truncated normal distribution (W2TND)
- mixture Weibull-Burr distribution (W2B3D)

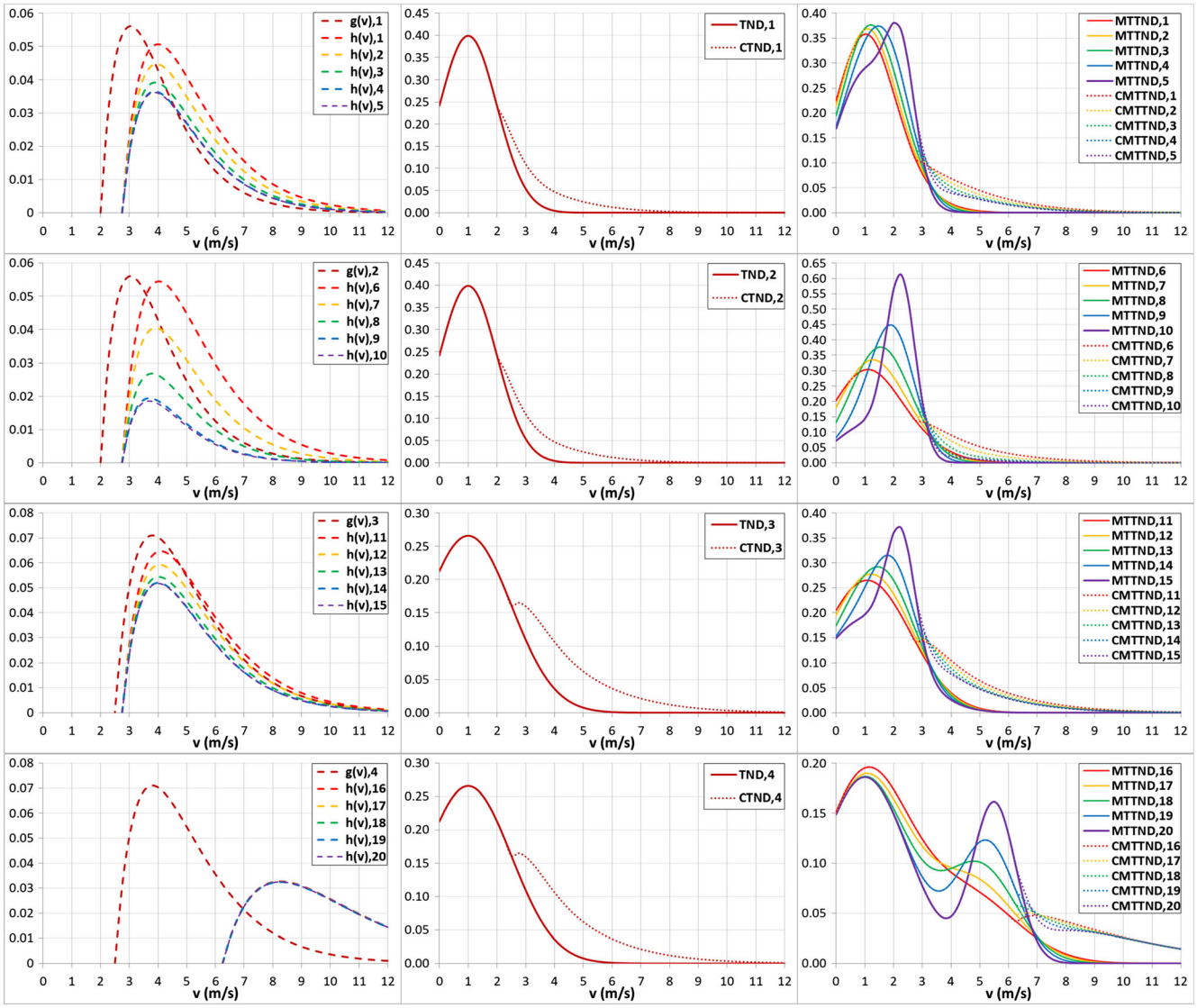

FIGURE 1 For different values of the parameters: on the left, functions $g(v)$ and $h(v)$; at the centre, TND and CTND; on the right, MTTNDs and CMTTNDs [Colour figure can be viewed at wileyonlinelibrary.com]

- mixture truncated normal–Burr distribution (TNB3D)
- mixture Burr-Burr distribution (B3B3D)
- mixture truncated normal–truncated normal distribution (MTTND)

The distributions considered, the characteristic parameters, the expressions of the PDFs and CDFs, and the domain of the random variable v are shown in Table 3.

The analytical expressions of the characteristic mean wind speeds of the different distributions are shown in Table 4.

2.4 | Estimation of the distribution parameters

As well established in the most relevant research papers,[8,15,20] the most used methods for the estimation of the distribution parameters are the moment method, maximum likelihood method, and least squares (LS) method. Among these ones, for all the PDFs considered in this article, the non-linear regression LS method, valid for both a single distribution and mixture distributions, was used. This permit to develop a uniform comparison among the distributions and localities considered.

The method consists in minimizing the residuals, namely, the sum of the squares of the difference between the data observed and data estimated by the analytical function. More details can be found in Mazzeo et al.[52] This method permits to overcome all problems deriving from the application of the maximum likelihood method that leads to strongly non-linear equations, which in the case of mixture distributions contain the sum of logarithms. In these cases, the unknown parameters are not

TABLE 3 – Distributions (W2D, TND, B3D, W2W2D, W2TND, W2B3D, TNB3D, B3B3D, and MTTND), parameters, analytical expressions of PDFs and CDFs, and domain

Distr.	Parameters	PDF $f(v)$	CDF $F(v)$	Domain
W2D	c scale k shape	$\frac{k}{c^k}v^{k-1}\exp\left[-\left(\frac{v}{c}\right)^k\right]$	$1-\exp\left[-\left(\frac{v}{c}\right)^k\right]$	$0 \le v < +\infty$
TND	μ scale σ shape	0 $\frac{1}{\sigma\sqrt{2\pi}}\exp\left[-\frac{(v-\mu)^2}{2\sigma^2}\right]$	0 $\frac{1}{2}\left[1+\operatorname{erf}\left(\frac{v-\mu}{\sqrt{2}\sigma}\right)\right]$	$-\infty < v < 0$ $0 \le v < +\infty$
B3D	β, t scale α shape	$\frac{\alpha t\left(\frac{v}{\beta}\right)^{\alpha-1}}{\beta\left[1+\left(\frac{v}{\beta}\right)^{\alpha}\right]^{t+1}}$	$1-\left[1+\left(\frac{v}{\beta}\right)^{\alpha}\right]^{-t}$	$0 \le v < +\infty$
W2W2D	w weight c_1,c_2 scale k_1,k_2 shape	$w_1\frac{k_1}{c_1}\left(\frac{v}{c_1}\right)^{k_1-1}\exp\left[-\left[\frac{v}{c_1}\right]^{k_1}\right]+w_2\frac{k_2}{c_2}\left(\frac{v}{c_2}\right)^{k_2-1}\exp\left[-\left[\frac{v}{c_2}\right]^{k_2}\right]$	$w_1\left\{1-\exp\left[-\left[\frac{v}{c_1}\right]^{k_1}\right]\right\}+w_2\left\{1-\exp\left[-\left[\frac{v}{c_2}\right]^{k_2}\right]\right\}$	$0 \le v < +\infty$
W2TND	w weight μ,c scale k, σ shape	0 $w_1\left\{\frac{1}{\sigma\sqrt{2\pi}}\exp\left[-\frac{[v-\mu]^2}{2\sigma^2}\right]\right\}+w_2\left\{\frac{k}{c}\left\{\frac{v}{c}\right\}^{k-1}\exp\left[-\left[\frac{v}{c}\right]^k\right]\right\}$	0 $w_1\left\{\frac{1}{2}\left[1+\operatorname{erf}\left[\frac{v-\mu}{\sqrt{2}\sigma}\right]\right]\right\}+w_2\left\{1-\exp\left[-\left[\frac{v}{c}\right]^k\right]\right\}$	$-\infty < v < 0$ $0 \le v < +\infty$
W2B3D	w weight c,β,t scale k,α shape	$w_1\left\{\frac{k}{c}\left\{\frac{v}{c}\right\}^{k-1}\exp\left[-\left[\frac{v}{c}\right]^k\right]\right\}+w_2\left\{\frac{\alpha t\left\{\frac{v}{\beta}\right\}^{\alpha-1}}{\beta\left[1+\left[\frac{v}{\beta}\right]^{\alpha}\right]^{t+1}}\right\}$	$w_1\left\{1-\exp\left[-\left[\frac{v}{c}\right]^k\right]\right\}+w_2\left\{1-\left[1+\left[\frac{v}{\beta}\right]^{\alpha}\right]^{-t}\right\}$	$0 \le v < +\infty$
TNB3D	w weight μ,β,t scale σ,α shape	0 $w_1\left\{\frac{1}{\sigma\sqrt{2\pi}}\exp\left[-\frac{[v-\mu]^2}{2\sigma^2}\right]\right\}+w_2\left\{\frac{\alpha t\left\{\frac{v}{\beta}\right\}^{\alpha-1}}{\beta\left[1+\left[\frac{v}{\beta}\right]^{\alpha}\right]^{t+1}}\right\}$	0 $w_1\left\{\frac{1}{2}\left[1+\operatorname{erf}\left[\frac{v-\mu}{\sqrt{2}\sigma}\right]\right]\right\}+w_2\left\{1-\left[1+\left[\frac{v}{\beta}\right]^{\alpha}\right]^{-t}\right\}$	$-\infty < v < 0$ $0 \le v < +\infty$
B3B3D	w weight β_1,β_2,t_1,t_2 scale α_1,α_2 shape	$w_1\left\{\frac{\alpha_1 t_1\left\{\frac{v}{\beta_1}\right\}^{\alpha_1-1}}{\beta_1\left[1+\left[\frac{v}{\beta_1}\right]^{\alpha_1}\right]^{t_1+1}}\right\}+w_2\left\{\frac{\alpha_2 t_2\left\{\frac{v}{\beta_2}\right\}^{\alpha_2-1}}{\beta_2\left[1+\left[\frac{v}{\beta_2}\right]^{\alpha_2}\right]^{t_2+1}}\right\}$	$w_1\left\{1-\left[1+\left[\frac{v}{\beta_1}\right]^{\alpha_1}\right]^{-t_1}\right\}+w_2\left\{1-\left[1+\left[\frac{v}{\beta_2}\right]^{\alpha_2}\right]^{-t_2}\right\}$	$0 \le v < +\infty$
MTTND	w weight μ_1,μ_2 scale σ_1,σ_2 shape	0 $w_1\left\{\frac{1}{\sigma_1\sqrt{2\pi}}\exp\left[-\frac{[v-\mu_1]^2}{2{\sigma_1}^2}\right]\right\}+w_2\left\{\frac{1}{\sigma_2\sqrt{2\pi}}\exp\left[-\frac{[v-\mu_2]^2}{2{\sigma_2}^2}\right]\right\}$	0 $w_1\left\{\frac{1}{2}\left[1+\operatorname{erf}\left[\frac{v-\mu_1}{\sqrt{2}\sigma_1}\right]\right]\right\}+w_2\left\{\frac{1}{2}\left[1+\operatorname{erf}\left[\frac{v-\mu_2}{\sqrt{2}\sigma_2}\right]\right]\right\}$	$-\infty < v < 0$ $0 \le v < +\infty$

TABLE 4 Analytical equations for the calculation of the characteristic mean wind speeds by means the conventional PDFs

Dist.	V_{m1}	$(V_{m2})^2$	$(V_{m3})^3$
W2D	$c\,\Gamma\left(1+\frac{1}{k}\right)$	$c^2\,\Gamma\left(1+\frac{2}{k}\right)$	$c^3\,\Gamma\left(1+\frac{3}{k}\right)$
TND	$\frac{\frac{\mu}{2}\left[1+\operatorname{erf}\left(\frac{\sqrt{2}\mu}{2\,\sigma}\right)\right]+\frac{\sigma}{\sqrt{2\pi}}\exp\left(-\frac{\mu^2}{2\sigma^2}\right)}{\frac{1}{2}\left[1+\operatorname{erf}\left(\frac{\sqrt{2}\mu}{2\,\sigma}\right)\right]}$	$\frac{\frac{1}{2}(\mu^2+\sigma^2)\left[1+\operatorname{erf}\left(\frac{\sqrt{2}\mu}{2\,\sigma}\right)\right]+\frac{\sigma\mu}{\sqrt{2\pi}}\exp\left(-\frac{\mu^2}{2\sigma^2}\right)}{\frac{1}{2}\left[1+\operatorname{erf}\left(\frac{\sqrt{2}\mu}{2\,\sigma}\right)\right]}$	$\frac{\frac{1}{2}\left[1+\operatorname{erf}\left(\frac{\sqrt{2}}{2}\left(\frac{\mu}{\sigma}\right)\right)\right](3\mu\sigma^2+\mu^3)+\frac{\sigma}{\sqrt{2\pi}}\exp\left(-\frac{\mu^2}{2\sigma^2}\right)^{(\mu^2+2\sigma^2)}}{\frac{1}{2}\left[1+\operatorname{erf}\left(\frac{\sqrt{2}\mu}{2\,\sigma}\right)\right]}$
B3D	$\frac{\beta\Gamma\left(1+\frac{1}{\alpha}\right)\Gamma\left(t-\frac{1}{\alpha}\right)}{\Gamma(t)}$	$\frac{\beta^2\Gamma\left(1+\frac{2}{\alpha}\right)\Gamma\left(t-\frac{2}{\alpha}\right)}{\Gamma(t)}$	$\frac{\beta^3\Gamma\left(1+\frac{3}{\alpha}\right)\Gamma\left(t-\frac{3}{\alpha}\right)}{\Gamma(t)}$
W2W2D	$w_1c_1\Gamma\left(1+\frac{1}{k_1}\right)+w_2c_2\Gamma\left(1+\frac{1}{k_2}\right)$	$w_1{c_1}^2\Gamma\left(1+\frac{2}{k_1}\right)+w_2{c_2}^2\Gamma\left(1+\frac{2}{k_2}\right)$	$w_1{c_1}^3\Gamma\left(1+\frac{3}{k_1}\right)+w_2{c_2}^3\Gamma\left(1+\frac{3}{k_2}\right)$
W2TND	$w_1c\,\Gamma\left(1+\frac{1}{k}\right)+w_2\frac{\frac{\mu}{2}\left[1+\operatorname{erf}\left(\frac{\sqrt{2}\mu}{2\,\sigma}\right)\right]+\frac{\sigma}{\sqrt{2\pi}}\exp\left(-\frac{\mu^2}{2\sigma^2}\right)}{\frac{1}{2}\left[1+\operatorname{erf}\left(\frac{\sqrt{2}\mu}{2\,\sigma}\right)\right]}$	$w_1c^2\,\Gamma\left(1+\frac{2}{k}\right)+w_2\frac{\frac{1}{2}(\mu^2+\sigma^2)\left[1+\operatorname{erf}\left(\frac{\sqrt{2}\mu}{2\,\sigma}\right)\right]+\frac{\sigma\mu}{\sqrt{2\pi}}\exp\left(-\frac{\mu^2}{2\sigma^2}\right)}{\frac{1}{2}\left[1+\operatorname{erf}\left(\frac{\sqrt{2}\mu}{2\,\sigma}\right)\right]}$	$w_1c^3\,\Gamma\left(1+\frac{3}{k}\right)+w_2\frac{\frac{1}{2}\left[1+\operatorname{erf}\left(\frac{\sqrt{2}}{2}\left(\frac{\mu}{\sigma}\right)\right)\right](3\mu\sigma^2+\mu^3)+\frac{\sigma}{\sqrt{2\pi}}\exp\left(-\frac{\mu^2}{2\sigma^2}\right)^{(\mu^2+2\sigma^2)}}{\frac{1}{2}\left[1+\operatorname{erf}\left(\frac{\sqrt{2}\mu}{2\,\sigma}\right)\right]}$
W2B3D	$w_1c\,\Gamma\left(1+\frac{1}{k}\right)+w_2\frac{\beta\Gamma\left(1+\frac{1}{\alpha}\right)\Gamma\left(t-\frac{1}{\alpha}\right)}{\Gamma(t)}$	$w_1{c_1}^2\Gamma\left(1+\frac{2}{k_1}\right)+w_2\frac{\beta^2\Gamma\left(1+\frac{2}{\alpha}\right)\Gamma\left(t-\frac{2}{\alpha}\right)}{\Gamma(t)}$	$w_1{c_1}^3\Gamma\left(1+\frac{3}{k_1}\right)+w_2\frac{\beta^3\Gamma\left(1+\frac{3}{\alpha}\right)\Gamma\left(t-\frac{3}{\alpha}\right)}{\Gamma(t)}$
TNB3D	$w_1\frac{\frac{\mu}{2}\left[1+\operatorname{erf}\left[\frac{\sqrt{2}\mu}{2\,\sigma}\right]\right]+\frac{\sigma}{\sqrt{2\pi}}\exp\left(-\frac{\mu^2}{2\sigma^2}\right)}{\frac{1}{2}\left[1+\operatorname{erf}\left[\frac{\sqrt{2}\mu}{2\,\sigma}\right]\right]}+w_2\frac{\beta\Gamma\left(1+\frac{1}{\alpha}\right)\Gamma\left(t-\frac{1}{\alpha}\right)}{\Gamma(t)}$	$w_1\frac{\frac{1}{2}(\mu^2+\sigma^2)\left[1+\operatorname{erf}\left[\frac{\sqrt{2}\mu}{2\,\sigma}\right]\right]+\frac{\sigma\mu}{\sqrt{2\pi}}\exp\left(-\frac{\mu^2}{2\sigma^2}\right)}{\frac{1}{2}\left[1+\operatorname{erf}\left[\frac{\sqrt{2}\mu}{2\,\sigma}\right]\right]}+w_2\frac{\beta^2\Gamma\left(1+\frac{2}{\alpha}\right)\Gamma\left(t-\frac{2}{\alpha}\right)}{\Gamma(t)}$	$w_1\frac{\frac{1}{2}\left[1+\operatorname{erf}\left[\frac{\sqrt{2}\mu}{2\,\sigma}\right]\right](3\mu\sigma^2+\mu^3)+\frac{\sigma}{\sqrt{2\pi}}\exp\left(-\frac{\mu^2}{2\sigma^2}\right)^{(\mu^2+2\sigma^2)}}{\frac{1}{2}\left[1+\operatorname{erf}\frac{\sqrt{2}\mu}{2\,\sigma}\right]}+w_2\frac{\beta^3\Gamma\left(1+\frac{3}{\alpha}\right)\Gamma\left(t-\frac{3}{\alpha}\right)}{\Gamma(t)}$
B3B3D	$w_1\frac{\beta_1\Gamma\left(1+\frac{1}{\alpha_1}\right)\Gamma\left(t_1-\frac{1}{\alpha_1}\right)}{\Gamma(t_1)}+w_2\frac{\beta_2\Gamma\left(1+\frac{1}{\alpha_2}\right)\Gamma\left(t_2-\frac{1}{\alpha_2}\right)}{\Gamma(t_2)}$	$w_1\frac{{\beta_1}^2\Gamma\left(1+\frac{2}{\alpha_1}\right)\Gamma\left(t_1-\frac{2}{\alpha_1}\right)}{\Gamma(t_1)}+w_2\frac{{\beta_2}^2\Gamma\left(1+\frac{2}{\alpha_2}\right)\Gamma\left(t_2-\frac{2}{\alpha_2}\right)}{\Gamma(t_2)}$	$w_1\frac{{\beta_1}^3\Gamma\left(1+\frac{3}{\alpha_1}\right)\Gamma\left(t_1-\frac{3}{\alpha_1}\right)}{\Gamma(t_1)}+w_2\frac{{\beta_2}^3\Gamma\left(1+\frac{3}{\alpha_2}\right)\Gamma\left(t_2-\frac{3}{\alpha_2}\right)}{\Gamma(t_2)}$

(Continues)

TABLE 4 (Continued)

Dist.	V_{m1}	$(V_{m2})^2$	$(V_{m3})^3$
MTTND	$\frac{\mu_1}{2}\left[1+\operatorname{erf}\left[\frac{\sqrt{2}\mu_1}{2\ \sigma_1}\right]\right]+\frac{\sigma_1}{\sqrt{2\pi}}\exp\left(-\frac{\mu_1^2}{2\sigma_1^2}\right)\frac{w_1A_1}{w_1A_1+w_2A_2}+\frac{\mu_2}{2}\left[1+\operatorname{erf}\left[\frac{\sqrt{2}\mu_2}{2\ \sigma_2}\right]\right]+\frac{\sigma_2}{\sqrt{2\pi}}\exp\left(-\frac{\mu_2^2}{2\sigma_2^2}\right)\frac{w_2A_2}{w_1A_1+w_2A_2}$	$\frac{1}{2}(\mu_1^2+\sigma_1^2)\left[1+\operatorname{erf}\left[\frac{\sqrt{2}\mu_1}{2\ \sigma_1}\right]\right]+\frac{\sigma_1\mu_1}{\sqrt{2\pi}}\exp\left(-\frac{\mu_1^2}{2\sigma_1^2}\right)\frac{w_1A_1}{w_1A_1+w_2A_2}+\frac{1}{2}(\mu_2^2+\sigma_2^2)\left[1+\operatorname{erf}\left[\frac{\sqrt{2}\mu_2}{2\ \sigma_2}\right]\right]+\frac{\sigma_2\mu_2}{\sqrt{2\pi}}\exp\left(-\frac{\mu_2^2}{2\sigma_2^2}\right)\frac{w_2A_2}{w_1A_1+w_2A_2}$	$\frac{1}{2}\left[1+\operatorname{erf}\left(\frac{\sqrt{2}\mu_1}{2\ \sigma_1}\right)\right](3\mu_1\sigma_1^2+\sigma_1^3)+\frac{\sigma_1}{\sqrt{2\pi}}\exp\left(-\frac{\mu_1^2}{2\sigma_1^2}\right)(\mu_1^2+2\sigma_1^2)\frac{w_1A_1}{w_1A_1+w_2A_2}+\frac{1}{2}\left[1+\operatorname{erf}\left(\frac{\sqrt{2}\mu_2}{2\ \sigma_2}\right)\right](3\mu_2\sigma_2^2+\sigma_2^3)+\frac{\sigma_2}{\sqrt{2\pi}}\exp\left(-\frac{\mu_2^2}{2\sigma_2^2}\right)(\mu_2^2+2\sigma_2^2)\frac{w_2A_2}{w_1A_1+w_2A_2}$

analytically calculable and a numerical and iterative approach is required.

To implement the non-linear LS method, the curve fitting toolbox of MATLAB[55] was used, which employs the iterative trust-region algorithm to determine the optimal distribution parameters after a number iterations starting from initial values set.

The tool requires as input the vector containing the values of the experimental discrete PDF for each wind speed class and the analytical PDF equation. In addition, permits to set some constraints on the parameters and a convergence criterion. As output, it provides the PDF parameters that lead to the minimization of the residuals.

2.5 | Goodness-of-fit and accuracy in the estimation of the characteristic mean wind speeds

Generally, the accuracy of distribution is quantified with correlation indices. This criterion makes it possible to evaluate the dispersion between the experimental relative frequencies and the estimated ones regardless of the wind speed value at the different classes. To evaluate the GOF of distributions considered, the statistical indices R^2 and RMSE, calculated for both the PDF and CDF, were used in this work. The R^2 measures the strength of the correlation between predicted and experimental distributions. Instead, RMSE quantifies the square root of the mean square of the differences between predicted and experimental distributions.

An excellent correlation between the analytical and experimental distribution does not ensure high accuracy in the calculation of the characteristic mean wind speeds. In fact, these mean wind speeds are dependent, in addition to the relative frequencies associated with the different wind speed classes, also on the corresponding values of wind speeds as evidenced by Equations (9a), (9b), and (9c). For this reason, in addition to the indices of GOF, the accuracy of the different distributions was evaluated by comparing the experimental and analytically calculated mean wind speeds.

The comparison was made by evaluating the relative percentage error, obtained through the following equation:

$$\varepsilon = 100\frac{V_{\mathrm{mr}} - V_{\mathrm{mr,exp}}}{V_{\mathrm{mr,exp}}}, \tag{30}$$

where V_{mr} indicates the mean wind speed of rth degree and $V_{\mathrm{mr,exp}}$ represents the corresponding value evaluated from the experimental data.

To identify the accuracy of distribution in the estimation of the characteristic mean wind speeds in different locations, it is necessary to use synthetic statistical indices of the relative error. For this reason, a box plot representation of the relative error was used. The fundamental parameters of a box plot are the mean value, the median value, and the interquartile range IQR_{13}, between the first and third quartiles. The distance between the first and the second quartile IQR_{12} and that between the second and the third quartile IQR_{23} allow the identification if the error distribution is symmetric. If these distances are different, for example, with $IQR_{12} < IQR_{23}$, any value of error lower than the median value is more frequent than any value of error greater than the median value. Vice versa for $IQR_{23} < IQR_{12}$. Consequently, if the median error is positive, an error less than the median error, closer to zero, is more probable when $IQR_{12} < IQR_{23}$, while if the median error is negative, an error greater than the median, closer to zero, is more probable when $IQR_{23} < IQR_{12}$.

The values of the relative errors obtained in the different locations were used to trace the box plots for each distribution and were summarized by means of a deterministic index, the mean value of the relative error, and a statistical dispersion index, namely, the interquartile range IQR_{13}. An accurate distribution in the estimation of characteristic mean wind speeds is characterized by a mean value of the relative error and by an IQR value close to zero.

2.6 | Case study

To verify the accuracy of the proposed CMTTND, as well as of the CTND, wind speed data in seven different locations were considered. For each location, the discrete PDFs and CDFs, as well as the experimental statistical characteristic quantities described in Section 2.1, were determined. Subsequently, the parameters of the different distributions were estimated using the non-linear regression LS method described in Section 2.4. Characteristic mean wind speeds were evaluated both by using the analytical equations, Equations (17), (20), and (23) for the CTND and the CMTTND and those reported in Table 4 for the conventional distributions, and the numerical integration method of Equations (9a), (9b), and (9c). The CMTTND accuracy, in the representation of the discrete distribution of the measured data and in the estimation of the characteristic mean wind speeds (V_{m1}, V_{m2}, and V_{m3}), was compared with that of the other PDFs through the statistical dispersion indices chosen in Section 2.5.

The wind speed data considered are related to four weather stations located along the Italian coasts at the sea level,[53] Ancona, Crotone, Messina, Porto Empedocle, and three inland American stations belonging to the National Renewable Energy Laboratory NREL.[54] One station is located in Las Vegas (Nevada) at an altitude of 523 m a.s.l. and the other two in Golden (Colorado), namely, the stations baseline measurement system (BMS) and rotating shadowband radiometer (RSR), at the same latitude, similar longitude and different altitudes, respectively, of 1829 m a.s.l. and 1793 m a.s.l. Table 5 shows the geographical location of the seven stations. The localities considered are characterized by different wind regimes:

- the discrete PDFs of Ancona and Messina show an accentuated bimodal trend with two maximum values with the first locality characterized by a greater frequency of CWS than the second one;
- Crotone has a slight bimodal trend with high relative frequencies at high wind speeds;
- Porto Empedocle has a slight bimodal trend with high CWS and high relative frequencies at high wind speeds;
- Nevada presents a unimodal trend with a high asymmetry with no CWS and a reduced variation range of wind speed;
- Colorado (BMS) presents a unimodal trend with a high asymmetry and CWS;
- Colorado (RSR) has a unimodal trend with a reduced variation range of wind speed and a high maximum relative frequency.

The experimental data refer to a period of 3 years: from 2012 to 2014 for the weather stations of Messina and Crotone and from 2014 to 2016 for the remaining stations. The wind speed data of the Italian locations are measured and summarized with a frequency of 10 minutes, while the data of the American stations are measured with a frequency of one minute. To make uniform the samples, wind speeds data were subsequently summarized with a frequency of 10 minutes by means of the mean value. All measurements were made at a height of 10 m.

For the calculation of the discrete PDF and CDF for each location, the wind speed domain was subdivided into classes of 0.5 m/s, with reference value the one relative to the centre of the class. Table 5 also shows the experimental characteristic quantities: mean wind speed V_{m1}, standard deviation σ, maximum wind speed V_{max}, wind speed at the highest relative frequency V_{fmax}, maximum relative frequency f_{max}, relative frequency at the CWS $f(0)$, mean square wind speed V_{m2}, mean cubic wind speed V_{m3}, and fisher asymmetry coefficient γ.

TABLE 5 Localities, geographical coordinates, and experimental characteristic quantities of discrete distributions and mean wind speeds

#	Location	Latitude L, ° Longitude l, °	V_{m1}, m/s	σ, m/s	V_{max}, m/s	V_{fmax}, m/s	f_{max}, $(m/s)^{-1}$	$f(0)$, $(m/s)^{-1}$	V_{m2}, m/s	V_{m3}, m/s	γ (–)
1	Ancona	$L = 43°37'29.16''$ $l = 13°30'23.46''$	3.173	2.231	18.7	0.75	0.221	0.024	3.878	4.491	1.014
2	Crotone	$L = 39°04'60.89''$ $l = 17°08'13.40''$	3.880	2.904	21.4	1.75	0.265	0.002	4.847	5.705	1.184
3	Messina	$L = 38°11'46.73''$ $l = 15°33'48.65''$	4.615	2.715	22.3	3.75	0.140	0.003	5.354	5.983	0.690
4	Nevada	$L = 36°3'36.00''$ $l = 115°4'48.00''$	2.051	1.716	12.75	0.75	0.360	0.000	2.674	3.232	1.395
5	Colorado (BMS)	$L = 39°44'31.20''$ $l = 105°10'48.00''$	3.186	2.336	24.531	2.25	0.247	0.033	3.951	4.706	1.550
6	Colorado (RSR)	$L = 39°44'31.60''$ $l = 105°10'30.50''$	2.475	1.258	13.909	2.25	0.391	0.021	2.776	3.073	1.057
7	Porto Empedocle	$L = 37°17'08.72''$ $l = 13°31'36.64''$	3.957	3.058	20.8	0.75	0.227	0.032	5.001	5.907	1.160

3 | RESULTS AND DISCUSSION

3.1 | Adaptation of distributions to the experimental data

3.1.1 | Comparison between the CMTTND and MTTND

Experimental wind speed data from the different locations were used to estimate the parameters that appear in the CMTTND and in the MTTND by using the nonlinear regression LS method. Table 6 shows the weight, mean, and variance values of the TND,1 and TND,2 that compose the MTTND and the related area subtended A_{II}, as well as the parameter K_{II} that appears in the CMTTND.

The high difference between the means μ_1 and μ_2 confirms the bimodal behaviour of the wind speed distribution in the localities Ancona, Crotone, Messina, and Porto Empedocle. The entity of bimodality is determined by the value of the weights and the variances. The high values of K_{II} for the locations Porto Empedocle, Colorado (BMS), Crotone, and Messina are owing to the higher value of the maximum wind speed, see Table 5, ie, the position of the inflexion point $v = (\mu_2 + \sigma_2)$ and the truncated area $(1 - A_{II})$; see Table 6.

Figure 2 shows, for the different locations, a comparison: in terms of PDF on the left and CDF on the right, between the CMTTND, the MTTND, and the discrete experimental distribution. The TND,1 and TND,2, and the $h(v)$ function are also shown in the image.

From the qualitative point of view, the figures show that the CMTTND adapts very well to the various PDFs and CDFs of discrete distributions, especially in locations with higher values of EWS and corresponding relative frequencies. Moreover, thanks to the correction made by the $h(v)$ function, the CDF reaches the unit value for all locations at high wind speeds.

3.1.2 | Comparison of the CTND and CMTTND with the conventional distributions

Experimental wind speed data were also used to estimate the parameters of the distributions W2D, TND, CTND, B3D, W2W2D, W2TND, W2B3D, TNB3D, and B3B3D, as described in Section 2.4. The values of the parameters obtained in the different locations are shown in Table 7. As for the CTND, in the same table, the value of the area subtended by the TND is also reported.

Figures 3 and 4 show a graphical comparison for the locations considered: on the left, between the proposed

TABLE 6 Parameters of the CMTTND and MTTND in the locations considered

Parametri	Ancona	Crotone	Messina	Nevada	Colorado (BMS)	Colorado (RSR)	Porto Empedocle
w_1	0.114	0.406	0.107	0.442	0.488	0.765	0.384
μ_1	0.786	1.659	1.367	0.944	2.359	2.167	1.817
σ_1	0.339	0.734	0.593	0.584	1.117	0.861	0.930
w_2	0.886	0.594	0.893	0.558	0.5121	0.235	0.616
μ_2	3.019	4.724	4.577	2.551	3.404	3.583	4.624
σ_2	1.967	2.825	2.554	1.662	2.887	1.595	3.162
A_{II}	0.944	0.967	0.966	0.942	0.931	0.993	0.946
K_{II}	1.404	1.691	1.632	1.269	1.692	1.040	1.868

and conventional PDFs and the discrete experimental PDF and, on the right, between the proposed and conventional CDFs and the discrete experimental CDF. In particular, Figure 3 regards the unimodal distributions, while Figure 4 the bimodal distributions.

The bimodal distributions are qualitatively more suitable to represent the different wind regimes considered.

A comparison of Tables 6 and 7 shows that the TND has lower area values lower than those of the MTTND, denoting that with the correct representation of the CWS is associated a lower accuracy in the estimation of the relative frequencies of the other wind speeds. The correction allows recovering this area for both distributions.

3.2 | Comparison of the CTND and CMTTND with the conventional distributions

3.2.1 | Goodness-of-fit

To estimate the accuracy of the CTND and CMTTND and of the other distributions in the representation of the experimental data, the statistical dispersion indices R^2 and RMSE were evaluated. The results obtained for the different locations are shown in Table 8. The indices were determined for both PDF, R^2_{PDF} and $RMSE_{PDF}$, and for the CDF, R^2_{CDF} and $RMSE_{CDF}$.

The table shows that

- in most cases, bimodal distributions have R^2 values higher and RMSE values lower than those obtained using unimodal distributions;
- the PDF and CDF of the CMTTND provide a very accurate representation, regardless of the wind regime, compared with the other distributions considered;
- the CMTTND is very accurate with R^2 values greater than 0.977 (except for the Nevada station where $R^2 = 0.917$) and RMSE values always lower than 0.054;
- the accuracy of the MTTND is comparable with that of the CMTTND, with an R^2 value of not less than 0.978 (except for the Nevada station where $R^2 = 0.914$) and RMSE values no higher than 0.071;
- the distributions that use only TNDs, ie, the TND, CTND, MTTND, and CMTTND, in the locality of Nevada, characterized by the absence of CWS, are less adequate than the other unimodal and bimodal distributions since for $v = 0$ it is defined and different from zero;
- the mixture TNB3D is the only one to have an R^2 never lower than 0.990, while the W2D, W2W2D, and W2B3D are the only ones with RMSE values always lower than 0.042.

3.2.2 | Accuracy in the estimation of the characteristic mean wind speeds

For the locations considered, the mean wind speed, mean square wind speed, and mean cubic wind speed were evaluated. These quantities were calculated both by analytical equations and by the numerical integration method. For the numerical method, reference was made to wind speed classes of amplitude 0.1 m/s, to reduce the error committed, considering the wind speed at the centre of the interval as reference wind speed.

Figure 5 shows the experimental values of V_{m1}, V_{m2}, and V_{m3} and those calculated considering the different distributions by using the analytical equations and numerical integration method. Each image is related to the different distributions by varying the localities on the horizontal axes, whose associated numbers are reported in Table 5.

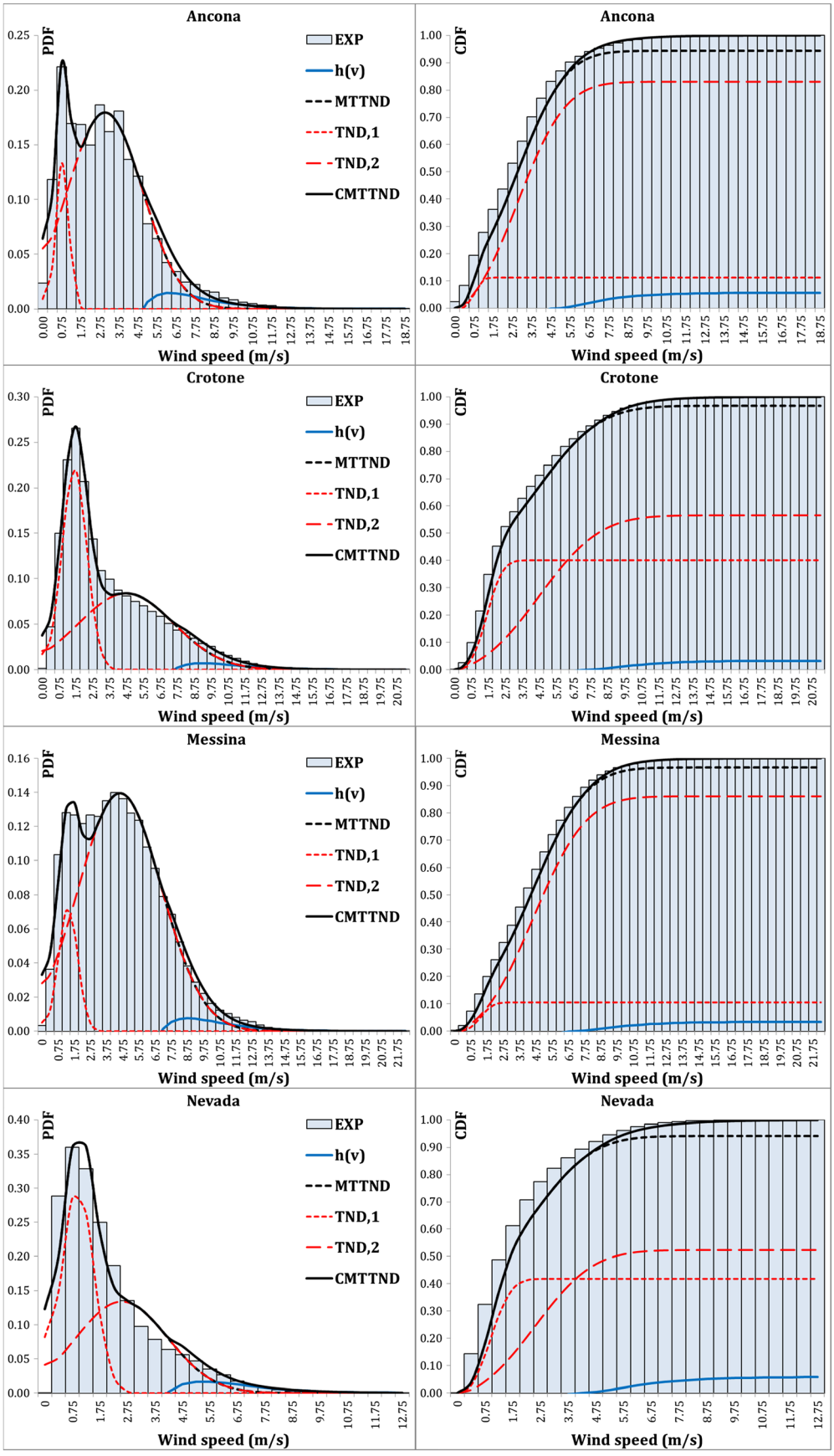

FIGURE 2 Comparison of MTTND and CMTTND in terms of PDF (left) and CDF (right). Contribution of TND,1, TND,2, and $h(v)$ [Colour figure can be viewed at wileyonlinelibrary.com]

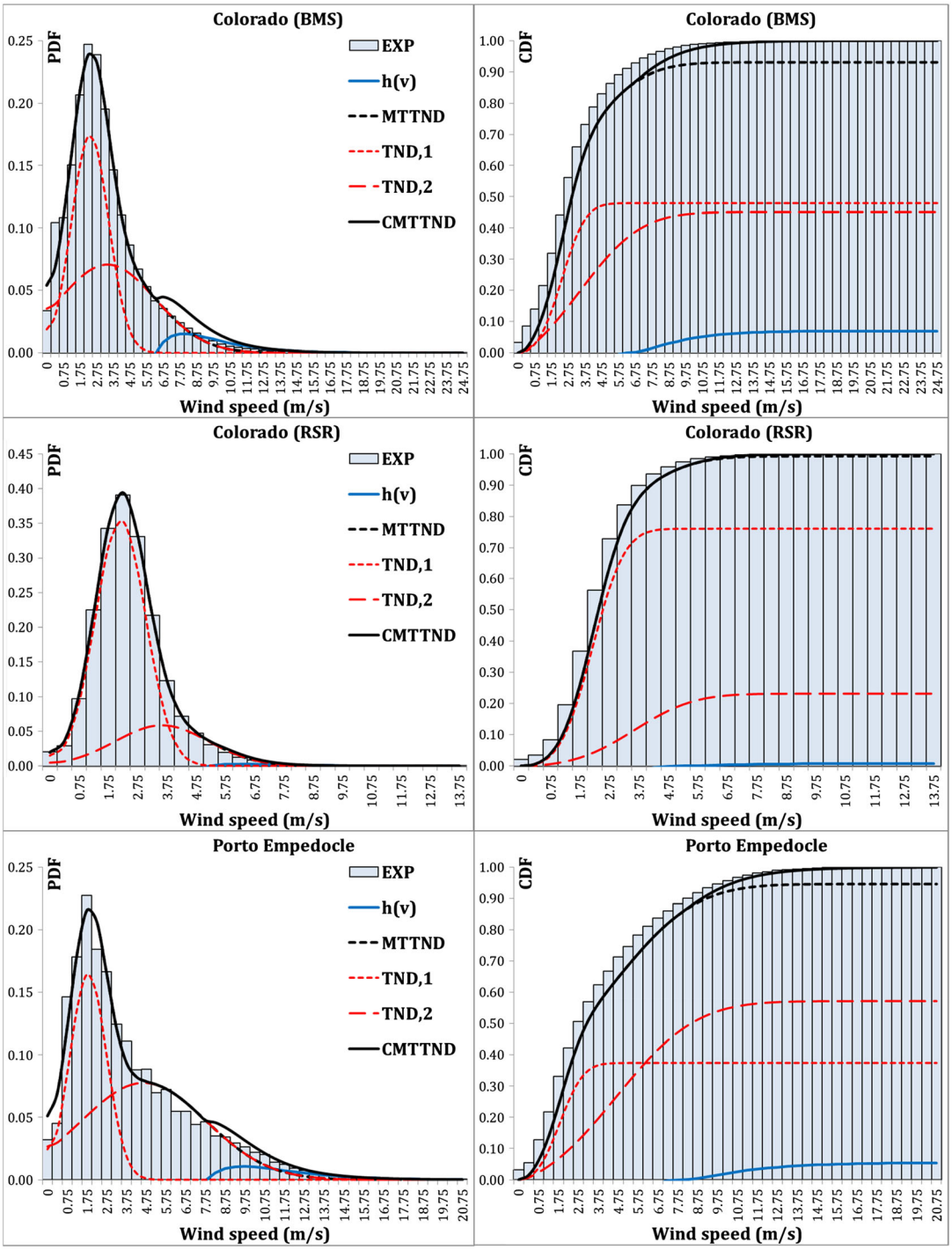

FIGURE 2 Continued.

The figure highlights that the wind speeds calculated analytically by means of the CMTTND and CTND overlap perfectly those calculated numerically. For this reason, the proposed analytical expressions, Equations (17), (20), and (23), can be considered validated. Analogously, for the analytical expressions of the other distributions, except for unimodal and bimodal distributions containing a Burr distribution, since a defined value is not always provided by the analytical equation. For the Burr distribution, the characteristic mean wind speeds of grade r can be calculated only when the condition $(t\alpha) > \beta$ is respected. When this condition is not respected, the analytical value, being undefined, was not reported in the images. Instead, when β and t tend to infinite, the BD coincides with the WD, and consequently, the characteristic mean wind speeds can be calculated directly the WD

TABLE 7 Parameter values of the PDFs in the locations considered

Distributions	Parameters	Ancona	Crotone	Messina	Nevada	Colorado (BMS)	Colorado (RSR)	Porto Empedocle
W2D	k	1.414	1.435	11.672	1.275	1.734	2.567	1.43
	c	3.721	3.783	5.355	2.125	3.529	2.684	4.141
TND	μ	2.534	2.334	4.051	1.31	2.559	2.282	2.478
	σ	2.167	2.237	2.823	1.267	1.759	1.019	2.448
CTND	μ	2.534	2.334	4.051	1.31	2.559	2.282	2.478
	σ	2.167	2.237	2.823	1.267	1.759	1.019	2.448
	K_I	1.56	1.6	1.82	1.17	1.34	0.83	1.69
	A_I	0.879	0.852	0.924	0.849	0.927	0.987	0.844
B3D	α	1.415	2.473	1.672	1.489	1.734	3.082	2.051
	β	318.6	1.771	237.3	2.852	282.6	3.185	2.534
	t	543.5	0.464	566.8	1.952	1998	2.017	0.7088
W2W2D	w_1	0.1425	0.2988	0.1323	0.2266	0.6862	0.4196	0.3234
	k_1	2.069	2.743	2.027	1.866	3.465	1.941	2.174
	c_1	0.8188	1.859	1.441	1.338	2.917	3.419	2.131
	w_2	0.8575	0.7012	0.8677	0.7734	0.7079	0.5804	0.6766
	k_2	1.95	1.58	2.18	1.18	1.32	3.21	1.6
	c_2	3.979	5.433	5.68	2.58	4.224	2.491	5.904
W2TND	w_1	0.1334	0.3025	0.7982	0.2113	0.6862	0.3429	0.3317
	μ	3.885	1.606	4.966	4.375	2.802	2.953	1.694
	σ	0.8431	0.6735	2.411	1.826	2.582	1.764	0.9466
	w_2	0.8666	0.6975	0.2018	0.7887	0.3138	0.6571	0.6683
	k	1.301	1.603	1.874	1.444	3.076	3.093	1.677
	c	3.455	5.404	2.001	1.627	2.711	2.473	5.771
W2B3D	w_1	0.8526	0.7013	0.8596	0.217	0.4329	0.4143	0.6541
	k	1.956	1.57	2.205	1.882	1.048	1.926	1.593
	c	3.99	5.433	5.704	1.333	3.567	3.425	6.024
	w_2	0.1474	0.2987	0.1404	0.783	0.5671	0.5857	0.3459
	α	2.207	2.782	2.09	1.192	3.981	3.216	2.254
	β	1.686	6.356	3.693	76.91	2.589	10.05	4.71
	t	5.312	30.82	7.183	58.27	0.68	88.72	6.029
TNB3D	w_1	0.6442	0.5045	0.6641	0.1355	0.8159	0.7347	1.311
	μ	3.322	5.285	5.036	4.86	2.411	2.117	1.61
	σ	1.714	2.975	2.307	1.6	1.366	0.8599	0.9111
	w_2	0.3558	0.4955	0.3359	0.8645	0.1841	0.2653	0.689
	α	2.823	2.61	2.248	1.454	9.181	3.408	1.905
	β	0.5653	2.715	1.638	7.258	5.264	4.383	8.555
	t	0.2465	2.372	0.5862	8.223	0.3045	1.764	2.63
B3B3D	w_1	0.5502	0.7007	0.6893	0.1034	0.4084	0.6225	0.4423
	α_1	3.346	1.584	2.768	6.079	1.076	3.425	2.893
	β_1	4.696	73.04	10.81	5.094	27.72	4.013	7.629
	t_1	1.83	61.61	5.574	0.9058	10.12	5.094	1.508
	w_2	0.4498	0.2993	0.3107	0.8966	0.5916	0.3775	0.5577
	α_2	2.28	2.765	2.158	1.448	4.004	1.86	2.063
	β_2	0.7753	7.315	1.668	6.459	2.555	8.691	4.859
	t_2	0.4214	44.54	0.8004	6.595	0.6298	6.383	4.726

equations. To be able to consider β and t values sufficiently high, the parameter $\beta/t^{(1/\alpha)}$ of the BD must be very close to the parameter c of the WD.

Owing to these issues, the sole method of numerical integration was used to make a complete comparison between the different distributions in the various localities considered. Instead, the analytical method was useful for the validation of the proposed expressions.

Figure 6 shows, respectively, the box plots, referring to the various locations, of the relative errors of the mean, mean square, and mean cubic wind speeds committed using the various distributions.

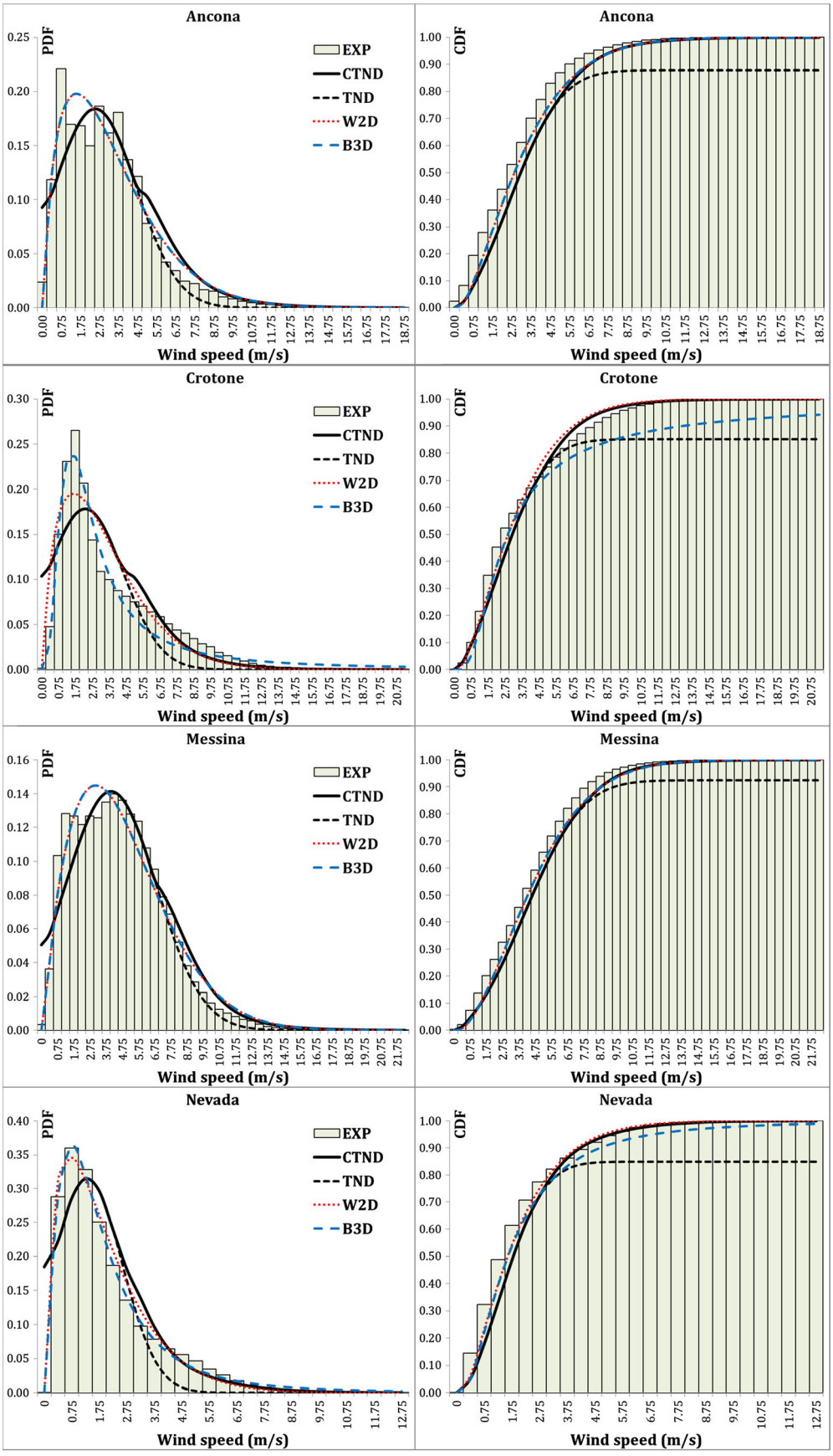

FIGURE 3 Comparison of the unimodal distributions (CTND, TND, W2D, and B3D) in terms of PDF (left) and CDF (right) [Colour figure can be viewed at wileyonlinelibrary.com]

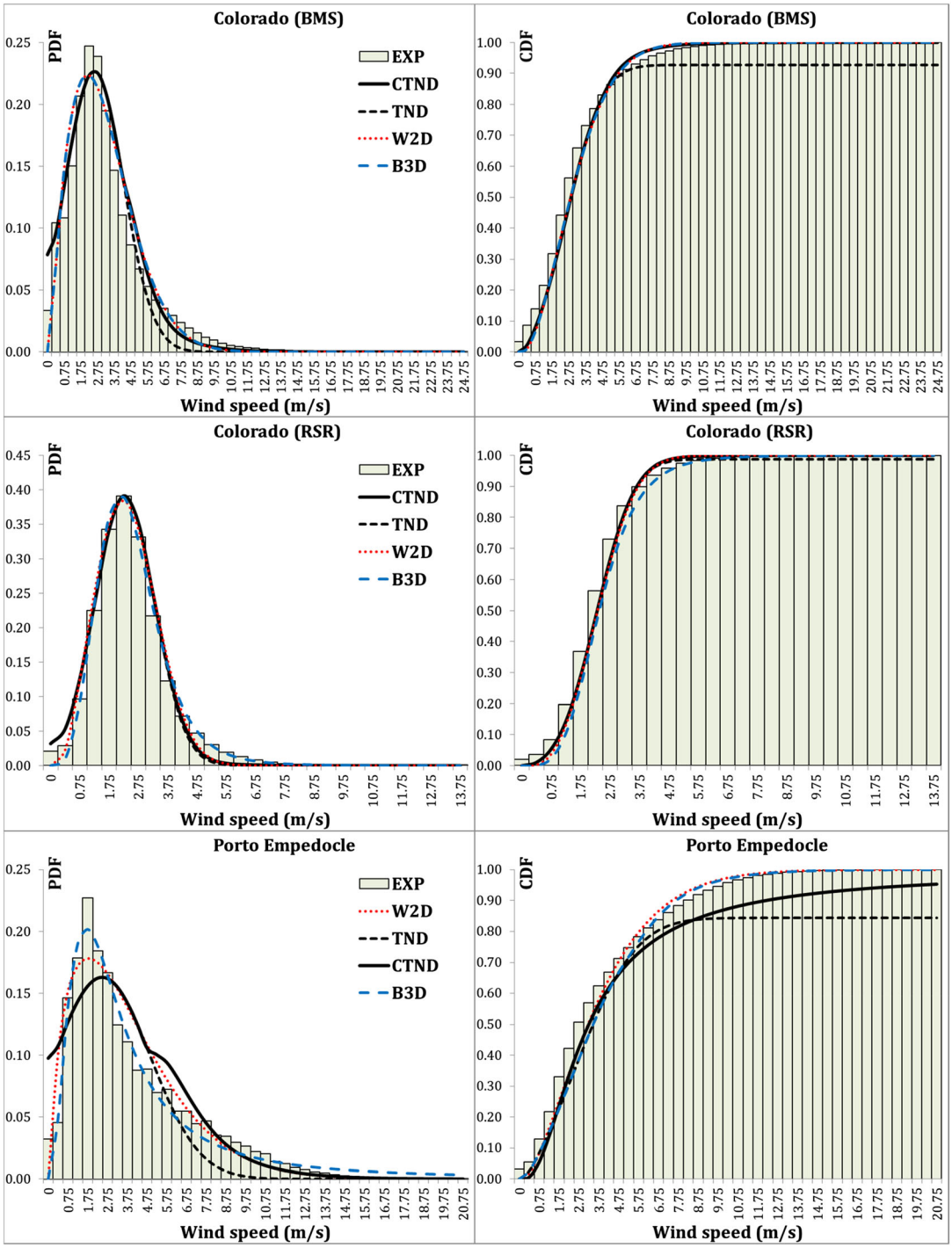

FIGURE 3 Continued.

Relative error of the mean wind speed

The image at the top shows that the mean wind speed is mainly overestimated by the distributions B3D, W2W2D, W2TND, W2B3D, TNB3D, B3B3D, and CMTTND, is mostly underestimated by the MTTND, and is always underestimated by the TND. W2D and CTND can lead to an underestimation or overestimation of the mean wind speed. The distributions with the lowest mean value of the relative error of the mean wind speed are the W2D with a value of −0.46%, MTTND with a value of −1.51%, and W2TND with a value of 1.96%. With these mean errors are also associated small interquartile ranges of the error, of about 4% to 5%. The minimum interquartile ranges are obtained by using the B3D and B3B3D with values around 3.5%, to which, however, the highest mean error values are associated, equal to about 6.5%. Consequently, the probability that the error committed by using B3D or B3B3D is equal to the mean error is greater. The

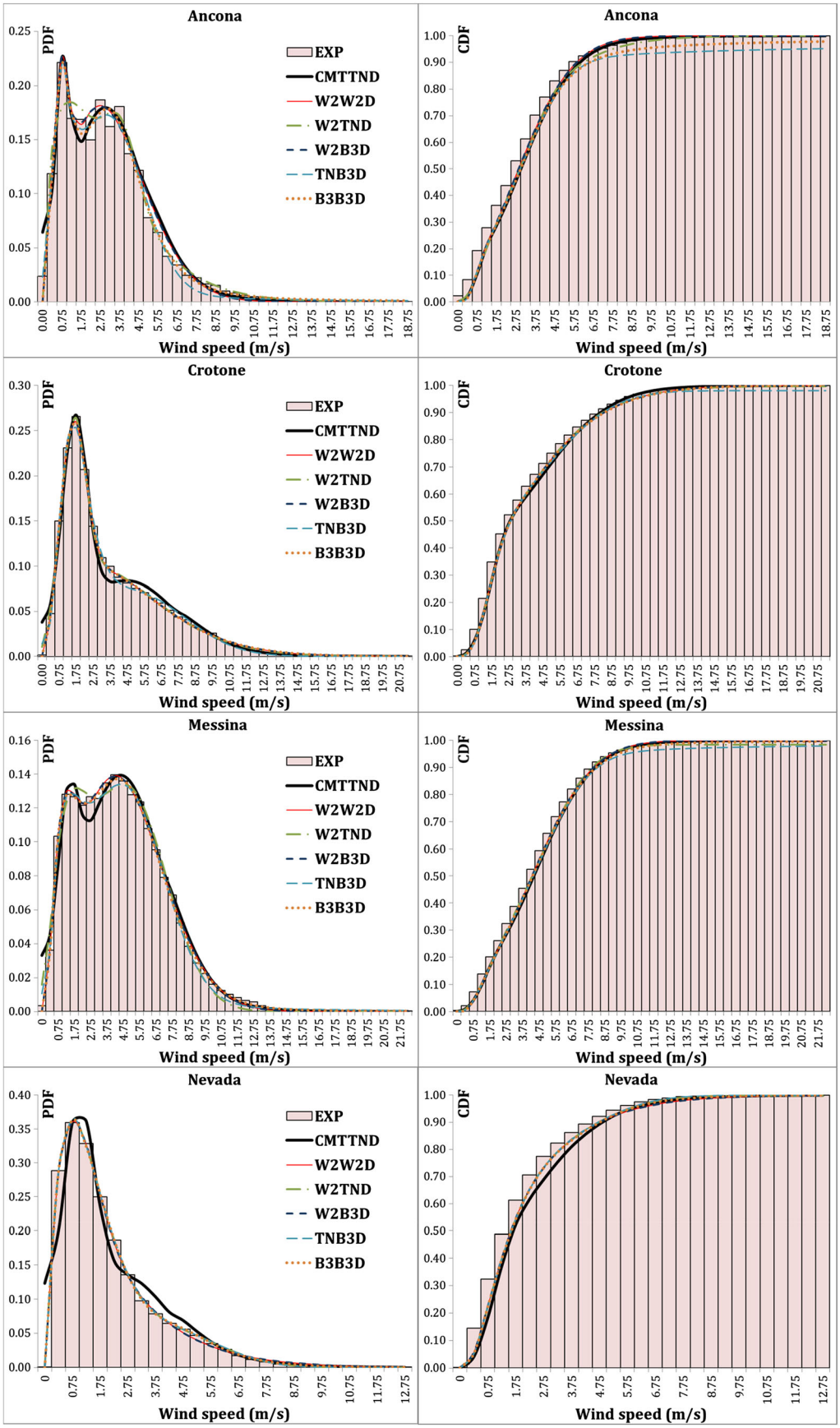

FIGURE 4 Comparison of the bimodal distributions (CMTTND, W2W2D, W2TND, W2B3D, TNB3D, and B3B3D) in terms of PDF (left) and CDF (right) [Colour figure can be viewed at wileyonlinelibrary.com]

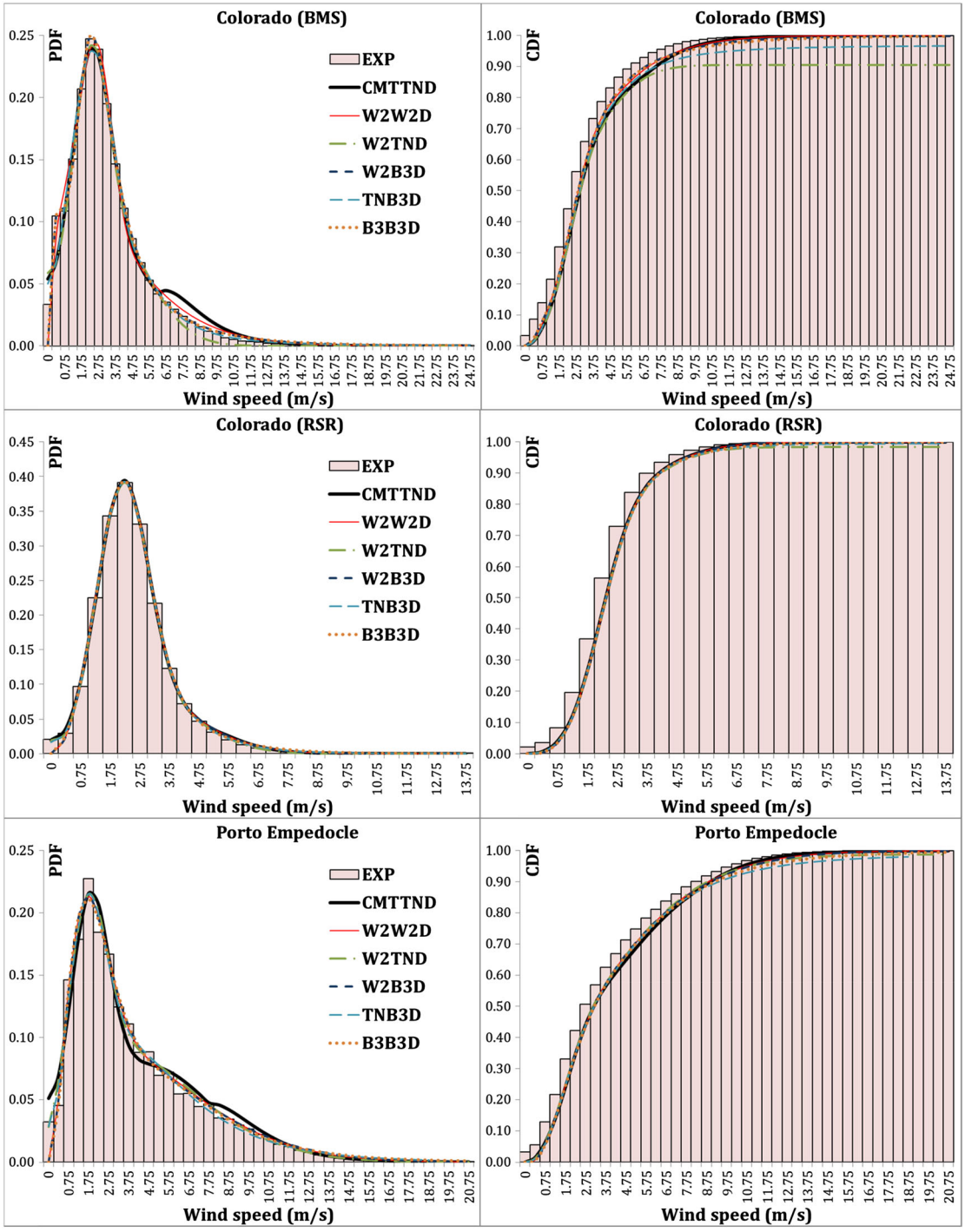

FIGURE 4 Continued.

B3D and W2D have the most asymmetric error distributions with $IQR_{12} << IQR_{23}$, while the W2TND, W2W2D, W2B3D, and TNB3D have the most asymmetric error distributions with $IQR_{23} << IQR_{12}$.

The error distribution of the CTND has a mean value of 3.23%, an IQR_{13} of 9.11%, an asymmetry with errors lower than the median value, with a value equal to 1.29%, more probable than errors higher than the median ($IQR_{12} < IQR_{23}$). The correction of the TND gives rise to a drastic reduction of the absolute value of the mean error of the mean wind speed (this error changes from a negative to a positive value); a substantial reduction of the IQR_{13}; and an inversion of the asymmetry of the error distribution.

The error distribution of the CMTTND has a mean value of 6.78%, an IQR_{13} of 7.61%, and an asymmetry with $IQR_{12} = 2.76\%$. The correction of MTTND gives rise to an increase in the absolute value of the mean error of

TABLE 8 Statistical dispersion indices R^2 and RMSE, related to the PDFs and CDFs in the locations considered

Stations	Indices	W2D	TND	CTND	B3D	W2W2D	W2TND	W2B3D	TNB3D	B3B3D	MTTND	CMTTND
Ancona	R^2_{PDF}	0.951	0.916	0.905	0.951	0.986	0.976	0.986	0.991	0.990	0.978	0.977
	R^2_{CDF}	0.995	0.996	0.989	0.995	0.998	0.998	0.998	0.999	0.998	0.997	0.996
	$RMSE_{PDF}$	0.015	0.020	0.022	0.015	0.009	0.011	0.009	0.007	0.007	0.010	0.011
	$RMSE_{CDF}$	0.040	0.110	0.059	0.040	0.031	0.033	0.031	0.055	0.044	0.055	0.037
Crotone	R^2_{PDF}	0.893	0.761	0.788	0.969	0.999	0.998	0.999	0.996	0.999	0.984	0.986
	R^2_{CDF}	0.992	0.971	0.990	0.994	0.998	0.998	0.998	0.999	0.998	0.998	0.998
	$RMSE_{PDF}$	0.022	0.033	0.030	0.012	0.002	0.003	0.002	0.004	0.002	0.008	0.008
	$RMSE_{CDF}$	0.029	0.112	0.034	0.072	0.023	0.022	0.023	0.026	0.023	0.032	0.024
Messina	R^2_{PDF}	0.975	0.951	0.948	0.975	0.999	0.993	0.999	0.998	0.999	0.986	0.987
	R^2_{CDF}	0.997	0.998	0.994	0.997	0.999	0.999	0.999	0.999	0.999	0.999	0.998
	$RMSE_{PDF}$	0.008	0.012	0.012	0.008	0.002	0.004	0.002	0.003	0.001	0.006	0.006
	$RMSE_{CDF}$	0.029	0.069	0.040	0.029	0.018	0.020	0.018	0.028	0.021	0.032	0.023
Nevada	R^2_{PDF}	0.990	0.823	0.838	0.998	0.999	1.000	0.999	1.000	1.000	0.914	0.917
	R^2_{CDF}	0.994	0.976	0.985	0.994	0.995	0.994	0.995	0.994	0.994	0.992	0.988
	$RMSE_{PDF}$	0.011	0.047	0.045	0.005	0.003	0.002	0.003	0.002	0.002	0.032	0.031
	$RMSE_{CDF}$	0.034	0.124	0.055	0.045	0.038	0.038	0.038	0.038	0.039	0.067	0.054
Colorado (BMS)	R^2_{PDF}	0.958	0.963	0.968	0.958	0.989	0.990	0.994	0.990	0.994	0.991	0.987
	R^2_{CDF}	0.996	0.992	0.996	0.996	0.996	0.997	0.996	0.997	0.996	0.998	0.992
	$RMSE_{PDF}$	0.014	0.014	0.013	0.014	0.007	0.007	0.005	0.007	0.005	0.006	0.008
	$RMSE_{CDF}$	0.031	0.063	0.030	0.031	0.037	0.090	0.036	0.054	0.037	0.071	0.046
Colorado (RSR)	R^2_{PDF}	0.989	0.989	0.990	0.995	0.998	1.000	0.998	1.000	0.999	1.000	1.000
	R^2_{CDF}	0.995	0.996	0.996	0.993	0.994	0.994	0.994	0.994	0.993	0.994	0.994
	$RMSE_{PDF}$	0.014	0.014	0.013	0.008	0.005	0.001	0.005	0.002	0.005	0.003	0.003
	$RMSE_{CDF}$	0.033	0.030	0.030	0.044	0.042	0.044	0.042	0.043	0.043	0.041	0.041
Porto Empedocle	R^2_{PDF}	0.928	0.843	0.858	0.975	0.986	0.989	0.986	0.990	0.986	0.978	0.979
	R^2_{CDF}	0.995	0.978	0.992	0.997	0.998	0.999	0.998	0.999	0.998	0.998	0.996
	$RMSE_{PDF}$	0.016	0.024	0.023	0.010	0.007	0.006	0.007	0.006	0.007	0.009	0.009
	$RMSE_{CDF}$	0.030	0.117	0.041	0.068	0.035	0.035	0.036	0.044	0.040	0.053	0.039

the mean wind speed (this error changes from a negative to a positive value), an invariance of the inequality $IQR_{12} < IQR_{23}$.

Relative error of the mean square wind speed

The image at the centre shows that the mean square wind speed is predominantly overestimated by the distributions B3D, W2W2D, W2B3D, TNB3D, and B3B3D, is always overestimated by the CMTTND, is predominantly underestimated by the W2D, and is always underestimated by the TND and MTTND. The CTND and W2TND can lead to an underestimation or overestimation of the mean square wind speed. The distributions with the lowest mean value of the relative error of the mean square wind speed are the CTND with a value of −0.03% and the W2TND with a value of 0.23%. With these, mean errors are associated interquartile ranges of the error of 11.02% and 4.17%, respectively. The minimum interquartile ranges are obtained by using the MTTND, W2TND, and B3B3D with values around 3% to 4%. However, the MTTND and B3B3D have high mean error values, respectively, of −4.85% and 7.59%. The W2D, CTND, and TNB3D have the most asymmetric error distributions with $IQR_{12} << IQR_{23}$, while the W2TND has the most asymmetric error distributions with $IQR_{23} << IQR_{12}$.

Regarding the error distribution of the CTND, $IQR_{12} = 3.36\%$. The correction of the TND gives rise to a drastic reduction of the absolute value of the mean error of the mean square wind speed, a significant reduction in the IQR_{13}, and an invariance of the asymmetry of the error distribution.

The error distribution of the CMTTND has a mean value of 5.46%, an IQR_{13} of 7.36%, and is approximately symmetric. The correction of MTTND gives rise to a slight increase in the absolute value of the mean error of the mean square wind speed (this error changes from a negative to a positive value), a substantial growth in the IQR_{13}, and a quasi-invariance of the symmetry of the error distribution.

Relative error of the mean cubic wind speed

The image at the bottom shows that the mean cubic wind speed is predominantly overestimated by the distributions

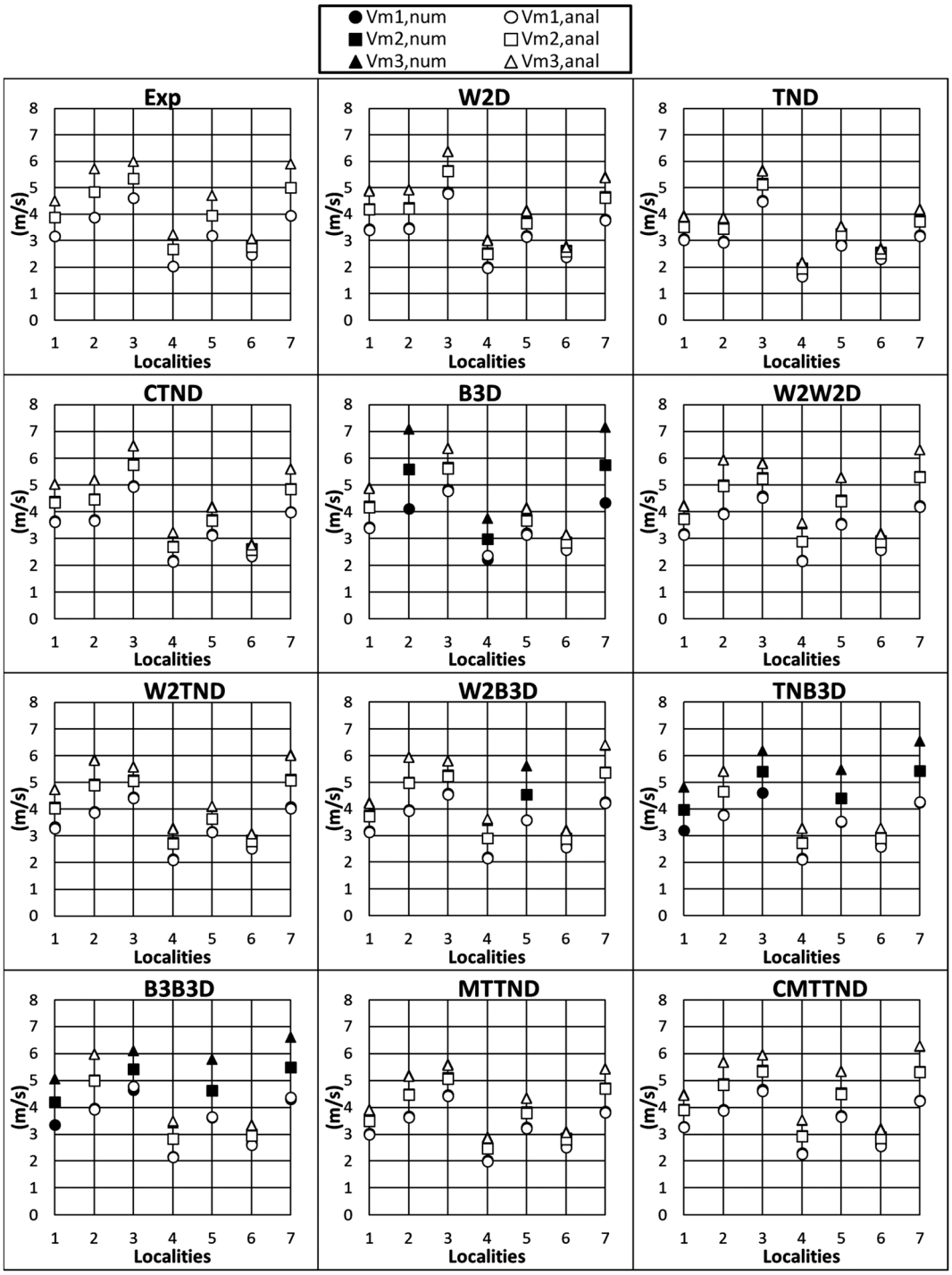

FIGURE 5 Experimental values and values calculated analytically and numerically with the different distributions of the mean wind speed V_{m1}, of the mean square wind speed V_{m2}, of the mean cubic wind speed V_{m3} in the different localities.

B3D, W2W2D, W2B3D, and TNB3D, is always overestimated by the B3B3D and CMTTND, is predominantly underestimated by the W2D, and is always underestimated by the TND and MTTND. The CTND and W2TND can lead to an underestimation or overestimation of the mean cubic wind speed. The distributions with the lowest mean value of the relative error of the mean cubic wind speed are the CTND with a value of −1.88% and the W2TND with a value of −0.84%. With these, mean errors are associated interquartile ranges of the error of 13.17% and 5.33%, respectively. The minimum interquartile range is obtained by using the MTTND with a value of 2.88%. However, the MTTND has high mean error values of −7.44%.

The W2D and CTND have the most asymmetric error distributions with $IQR_{12} << IQR_{23}$, while the W2TND

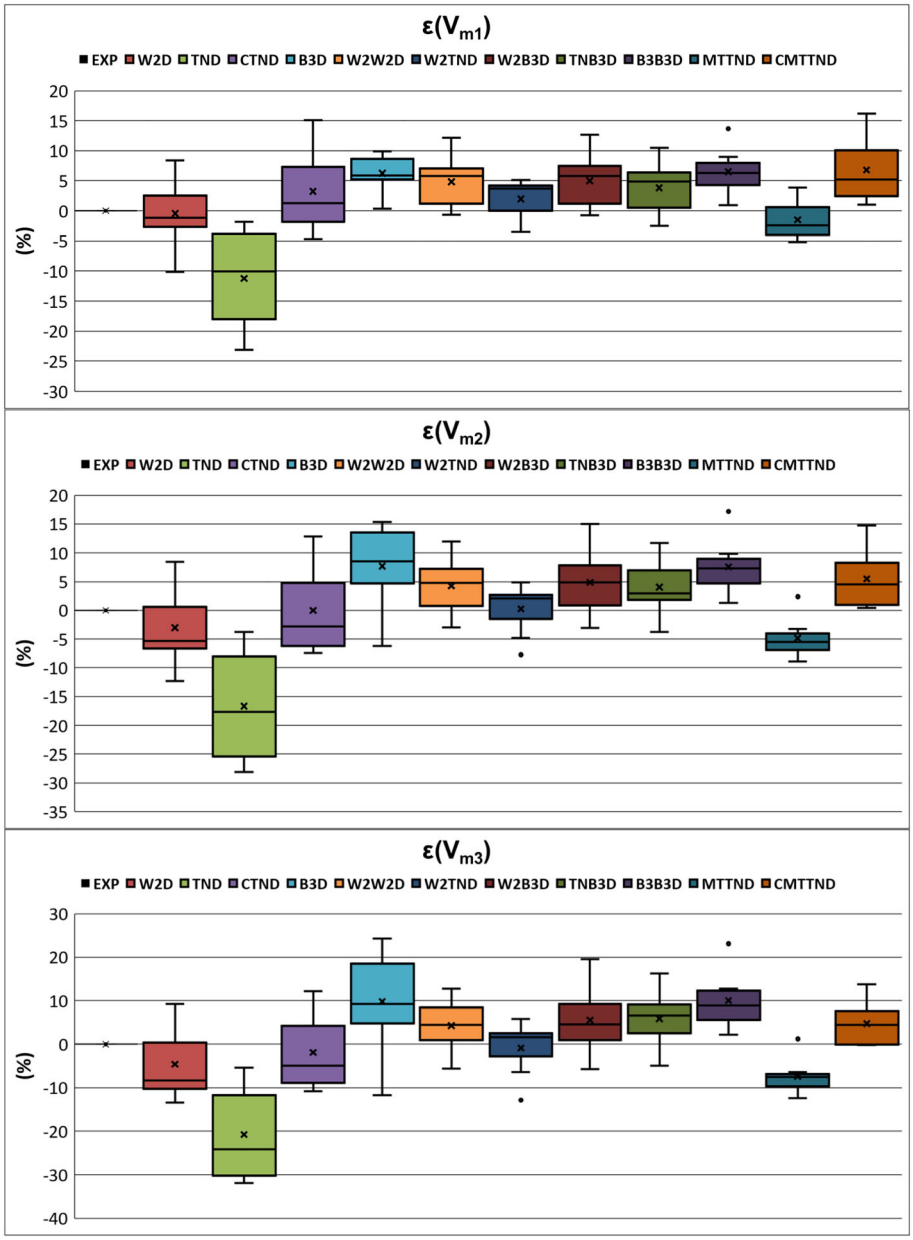

FIGURE 6 Box plots of the relative error of the mean wind speed, mean square wind speed, and mean cubic wind speed for the various distributions. [Colour figure can be viewed at wileyonlinelibrary.com]

and MTTND have the most asymmetric error distributions with $IQR_{23} << IQR_{12}$.

The correction of the TND gives rise to a drastic reduction of the absolute value of the mean error of the mean cubic wind speed, a significant reduction of the IQR_{13}, and an invariance of the asymmetry of the error distribution.

The error distribution of the CMTTND has a mean value of 4.73% and an IQR_{13} of 7.68% and is approximately symmetric. The correction of the MTTND gives rise to a significant reduction in the absolute value of the mean error of the mean cubic wind speed (this error changes from a negative to a positive value), a substantial growth of the IQR_{13}, and a quasi-invariance of the symmetry of the error distribution.

The subsequent analysis allows verifying for which wind regimes the correction should be carried out. Figure 7 shows the comparison between the experimental wind speeds and those obtained with the different distributions for the different locations considered. In the analysis, a limit percentage error of 10% was used to discriminate the different distributions.

The distributions that show a relative error in all seven locations below 10% are for the mean wind speed, the B3D, W2TND, and MTTND, for the mean square wind speed, the W2TND and MTTND, while for the mean

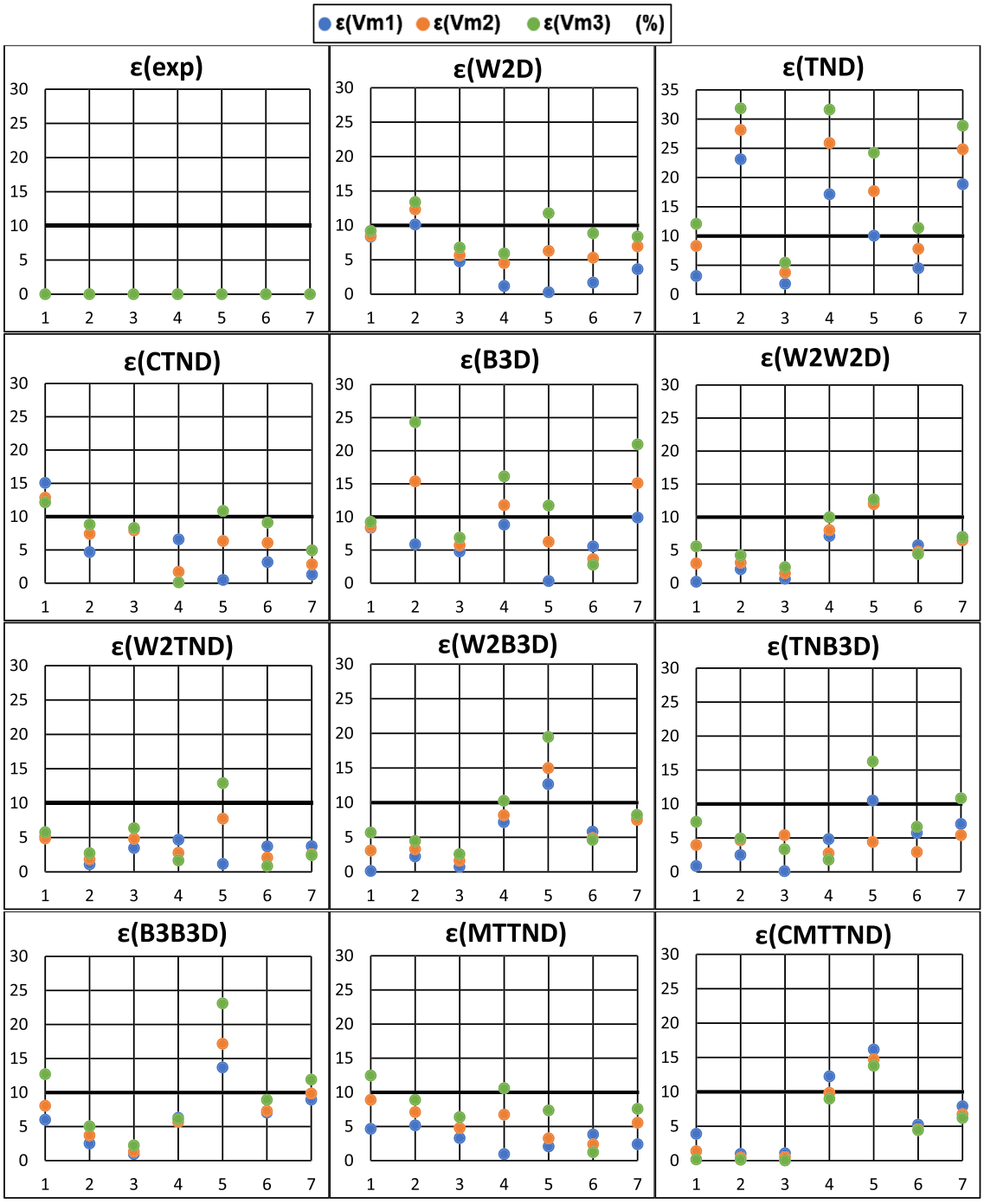

FIGURE 7 $\varepsilon(V_{m1})$, $\varepsilon(V_{m2})$, and $\varepsilon(V_{m3})$ for the different distribution in the various localities considered [Colour figure can be viewed at wileyonlinelibrary.com]

cubic wind speed no one. For the mean cubic wind speed, the W2W2D, W2TND, and CMTTND have values lower than 10% in six locations.

The CMTTND has the largest number of locations, three, where the relative error of the mean square and cubic wind speed is less than 2%. Instead, by using CMTTND, the relative error of the mean wind speed is less than 2% in two locations. Only the W2D has three locations with a relative error of less than 2%.

The correction of TND leads to greater accuracy in all locations except Ancona and Messina, while the correction of MTTND is improving in the localities of Ancona, Crotone, and Messina. Overall, the CMTTND distribution was the most appropriate and accurate in Ancona,

Crotone, and Messina, the CTND in Nevada, MTTND in Colorado (BMS), and the W2TND in Colorado (RSR) and Porto Empedocle.

4 | CONCLUSIONS

A correction of the truncated normal distribution and the mixture of two truncated normal distributions is proposed in this paper to estimate wind availability in a locality. The proposed distributions, in addition to taking into account the CWS, are able to predict the relative frequencies of the EWS. The proposed distributions CMTTND and CTND, by varying the characteristic parameters, have shown high flexibility to represent wind regimes characterized by the presence of CWS and EWS, as well as unimodal and bimodal trends.

The results of the comparison with the most common unimodal and bimodal distributions, in locations characterized by different wind regimes, showed the high GOF of the PDF and CDF of the CMTTND and CTND.

In all locations, the analytical equations proposed for the CTND and the CMTTND for the calculation of the mean characteristic wind speeds were validated since they provided results very close to those obtained using a numerical procedure.

For the proposed distributions, the relative error committed in the estimation of the mean characteristic wind speeds is reduced by increasing their degree, confirming that a more accurate estimation of the EWS is required. Consequently, by increasing the mean wind speed degree, the EWS correction has even more weight even if they present reduced relative frequencies.

In general, the use of CTND and CMTTND can lead to a more or less accurate estimation of mean characteristic wind speeds compared with the TND and MTTND in relation to the considered location, ie, to the wind regime. The analysis of the relative errors has shown that, in order to obtain a greater accuracy than the incorrect distributions, the CTND must be used in the localities where the statistical distribution of the wind speed has a unimodal character, while the CMTTND must be used in the localities in which the statistical distribution of wind speed has a bimodal character. In these locations, in general, the two distributions are the most accurate even with respect to all the distributions considered in this study.

Owing to the advantages demonstrated by the correction made in this work to unimodal and bimodal truncated normal distributions, future research works will permit to extend the distribution proposed also for multi-peak distributions by considering a mixture of three or more truncated normal distributions.

NOMENCLATURE

Abbreviations

BMS	baseline measurement system
CDF	cumulative density function
CMTTND	corrected mixture of two truncated normal distributions
CWS	calm wind speeds
CTND	corrected truncated normal distribution
DMWS	daily maximum wind speeds
EWS	extreme wind speeds
GOF	goodness-of-fit
MEP	maximum entropy principle
MMWS	maximum monthly wind speeds
MTTND	mixture of two truncated normal distributions
ND	normal distribution
NREL	national renewable energy laboratory
PDF	probability density function
RSR	rotating shadowband radiometer
TND	truncated normal distribution
TND,1	first TND of the MTTND
TND,2	second TND of the MTTND
YMWS	yearly maximum wind speeds

Symbols

A_0	frontal area traced by the wind turbine (m^2)
A_I	area subtended by the TND
A_{II}	area subtended by the MTTND
E_a	available energy (J)
$f(v)$	probability density function (s/m)
$f(V_i)$	discrete probability density distribution (s/m)
$F(v)$	cumulative density function
$g(v)$	corrective function of the CTND (s/m)
$h(v)$	corrective function of the CMTTND (s/m)
IQR_{12}	interquartile range between the first and second quartile (m/s)
IQR_{13}	interquartile range between the first and third quartile (m/s)
IQR_{23}	interquartile range between the second and third quartile (m/s)
K_I	extreme wind speed parameter of the CTND (m/s)
K_{II}	extreme wind speed parameter of the CMTTND (m/s)
l	longitude (°)
L	latitude (°)
N	number of wind speed observations

P_a	available mean power (W)
R^2	coefficient of determination
RMSE	root mean square error
V	wind speed observation (m/s)
v	wind speed aleatory variable (m/s)
V_{m1}	mean wind speed (m/s)
V_{m2}	mean square wind speed (m/s)
V_{m3}	mean cubic wind speed (m/s)
w	weight of a mixture distribution
T	observation period (s)

Greek symbols

ε	relative percentage error (%)
ΔV_{m1}	mean wind speed correction (m/s)
ΔV_{m2}	mean square wind speed correction (m/s)
ΔV_{m3}	mean cubic wind speed correction (m/s)
Δt	time interval (s)
μ	mean of a TND (m/s)
ρ	air density (kg/m^3)
σ	standard deviation (m/s)
γ	Fisher coefficient of skewness (-)
ξ	integration aleatory variable (m/s)

Subscripts

1	referring to the TND,1
2	referring to the TND,2
anal	referring to the analytical procedure
CDF	referring to the CDF
CMTTND	referring to the CMTTND
CTND	referring to the CTND
exp	experimental
fmax	referring to the maximum value of the discrete probability density distribution
i	ith wind speed observation
MTTND	referring to the MTTND
max	referring to the maximum value
mr	referring to the rth degree of the mean wind speed
num	referring to the numerical procedure
PDF	referring to the PDF
TND	referring to the TND

ORCID

Domenico Mazzeo https://orcid.org/0000-0001-7253-2506

REFERENCES

1. Akpinar S, Akpinar EK. Estimation of wind energy potential using finite mixture distribution models. *Energ Conver Manage*. 2009;50(4):877-884.
2. Pishgar-Komleh SH, Keyhani A, Sefeedpari P. Wind speed and power density analysis based on Weibull and Rayleigh distributions (a case study: Firouzkooh county of Iran). *Renew Sustain Energy Rev*. 2015;42:313-322.
3. Paraschiv L-S, Paraschiv S, Ion IV. Investigation of wind power density distribution using Rayleigh probability density function. *Energy Procedia*. 2019;157:1546-1552.
4. Usta I. An innovative estimation method regarding Weibull parameters for wind energy applications. *Energy*. 2016;106:301-314.
5. Costa Rocha PA, de Sousa RC, de Andrade CF, da Silva MEV. Comparison of seven numerical methods for determining Weibull parameters for wind energy generation in the northeast region of Brazil. *Appl Energy*. 2012;89(1):395-400.
6. Katinas V, Gecevicius G, Marciukaitis M. An investigation of wind power density distribution at location with low and high wind speeds using statistical model. *Appl Energy*. 2018;218:442-451.
7. Soulouknga MH, Doka SY, Revanna N, Djongyang N, Kofane TC. Analysis of wind speed data and wind energy potential in Faya-Largeau, Chad, using Weibull distribution. *Renew Energy*. 2018;121:1-8.
8. Carta JA, Ramírez P, Velázquez S. A review of wind speed probability distributions used in wind energy analysis case studies in the Canary Islands. *Renew Sustain Energy Rev*. 2009;13(5):933-955.
9. Zhou J, Erdem E, Li G, Shi J. Comprehensive evaluation of wind speed distribution models: a case study for North Dakota sites. *Energ Conver Manage*. 2010;51(7):1449-1458.
10. Wu J, Wang J, Chi D. Wind energy potential assessment for the site of Inner Mongolia in China. *Renew Sustain Energy Rev*. 2013;21:215-228.
11. Alavi O, Mohammadi K, Mostafaeipour A. Evaluating the suitability of wind speed probability distribution models: a case of study of east and southeast parts of Iran. *Energ Conver Manage*. 2016;119:101-108.
12. Kantar YM, Usta I, Arik I, Yenilmez I. Wind speed analysis using the extended generalized Lindley distribution. *Renew Energy*. 2018;118:1024-1030.
13. Aries N, Boudia SM, Ounis H. Deep assessment of wind speed distribution models: a case study of four sites in Algeria. *Energ Conver Manage*. 2018;155:78-90.
14. Masseran N. Integrated approach for the determination of an accurate wind-speed distribution model. *Energ Conver Manage*. 2018;173:56-64.
15. Kantar YM, Usta I. Analysis of the upper-truncated Weibull distribution for wind speed. *Energ Conver Manage*. 2015;96:81-88.
16. Abbas K, Alamgir KSA, Ali A, Khan DM, Khalil U. Statistical analysis of wind speed data in Pakistan. *World Appl Sci J*. 2012;18(11):1533-1539.

17. Soukissian T. Use of multi-parameter distributions for offshore wind speed modeling: The Johnson SB distribution. *Appl Energy*. 2013;111:982-1000.
18. Chang TP. Estimation of wind energy potential using different probability density functions. *Appl Energy*. 2011;88(5):1848-1856.
19. Ouarda TBMJ, Charron C, Shin J, et al. Probability distributions of wind speed in the UAE. *Energ Conver Manage*. 2015;93:414-434.
20. Ouarda TBMJ, Charron C. On the mixture of wind speed distribution in a Nordic region. *Energ Conver Manage*. 2018;174:33-44.
21. Hu Q, Wang Y, Xie Z, Zhu P, Yu D. On estimating uncertainty of wind energy with mixture of distributions. *Energy*. 2016;112:935-962.
22. Jung C, Schindler D, Laible J, Buchholz A. Introducing a system of wind speed distributions for modeling properties of wind speed regimes around the world. *Energ Conver Manage*. 2017;144:181-192.
23. Jung C, Schindler D. Sensitivity analysis of the system of wind speed distributions. *Energ Conver Manage*. 2018;177:376-384.
24. Shin J-Y, Ouarda TBMJ, Lee T. Heterogeneous mixture distributions for modeling wind speed, application to the UAE. *Renew Energy*. 2016;91:40-52.
25. Miao S, Gu Y, Li D, Li H. Determining suitable region wind speed probability distribution using optimal score-radar map. *Energ Conver Manage*. 2019;183:590-603.
26. Feijóo A, Villanueva D. Assessing wind speed simulation methods. *Renew Sustain Energy Rev*. 2016;56:473-483.
27. Jung C, Schindler D. Global comparison of the goodness-of-fit of wind speed distributions. *Energ Conver Manage*. 2017;133:216-234.
28. Takle ES, Brown JM. Note on the use of Weibull statistics to characterize wind speed data. *J Appl Meteorol*. 1978;17(4, Apr. 1978):556-559.
29. Bardsley WE. Note on the use of the inverse Gaussian distribution for wind energy applications. *J APPL METEROL*. 1980;19:1126-1130.
30. Carta JA, Ramírez P, Velázquez S. Influence of the level of fit of a density probability function to wind-speed data on the WECS mean power output estimation. *Energ Conver Manage*. 2008;49(10):2647-2655.
31. Qin X, Zhang J-S, Yan X-D. Two improved mixture Weibull models for the analysis of wind speed data. *J Appl Meteorol Climatol*. 2012;51(7):1321-1332.
32. Carta JA, Ramírez P. Analysis of two-component mixture Weibull statistics for estimation of wind speed distributions. *Renew Energy*. 2007;32(3):518-531.
33. Chiodo E, De Falco P. Inverse Burr distribution for extreme wind speed prediction: genesis, identification and estimation. *Electr Pow Syst Res*. 2016;141:549-561.
34. Castillo E. *Extreme Value Theory in Engineering*. 389 Boston, USA: Academic Press; 1988.
35. Akgül FG, Senoglu B, Arslan T. An alternative distribution to Weibull for modeling the wind speed data: inverse Weibull distribution. *Energ Conver Manage*. 2016;114:234-240.
36. Dukes MDG, Palutikof JP. Estimation of extreme wind speeds with very long return periods. *J Appl Meteorol*. 1995;34(9):1950-1961.
37. Simiu E, Heckert NA. Extreme wind distribution tails: a "peaks over threshold" approach. *J Struct Eng*. 1996;122(5):539-547.
38. Heckert NA, Simiu E, Whalen T. Estimates of hurricane wind speeds by "peaks over threshold" method. *J Struct Eng*. 1998;124(4):445-449.
39. Simiu E, Heckert NA, Filliben JJ, Johnson SK. Extreme wind load estimates based on the Gumbel distribution of dynamic pressures: an assessment. *Struct Saf*. 2001;23(3):221-229.
40. Perrin O, Rootzén H, Taesler R. A discussion of statistical methods used to estimate extreme wind speeds. *Theor Appl Climatol*. 2006;85(3-4):203-215.
41. Lee B-H, Ahn D-J, Kim H-G, Ha Y-C. An estimation of the extreme wind speed using the Korea wind map. *Renew Energy*. 2012;42:4-10.
42. Kang D, Ko K, Huh J. Determination of extreme wind values using the Gumbel distribution. *Energy*. 2015;86:51-58.
43. Morgan EC, Lackner M, Vogel RM, Baise LG. Probability distributions for offshore wind speeds. *Energ Conver Manage*. 2011;52(1):15-26.
44. Raynal J, Guevara J. Maximum likelihood estimators for the two populations Gumbel distribution. *Hydrol Sci Technol*. 1997;13:47-56.
45. Raynal J, Santillan O. Maximum likelihood estimators of the parameters of the mixed GEV distribution. IX Congresso Nacional de Hidràulica, AMH, Querétaro, Qro., Mexico; 1986, 79-90 p.
46. Escalante-Sandoval C. Application of bivariate extreme value distribution to flood frequency analysis: a case study of Northwestern Mexico. *Nat Hazards*. 2007;42(1):37-46.
47. Agustín ESC. Estimation of extreme wind speeds by using mixed distributions. *Ingeniería, Investigación y Tecnología*. 2013;14(2):153-162.
48. Rossi F, Fiorentino M, Versace P. Two-component extreme value distribution for flood frequency analysis. *Water Resour Res*. 1984;20(7):847-856.
49. de Waal DJ, van Gelder PHAJM, Beirlant J. Joint modelling of daily maximum wind strengths through the multivariate Burr-Gamma distribution. *J Wind Eng Ind Aerodyn*. 2004;92(12):1025-1037.
50. Baran S. Probabilistic wind speed forecasting using Bayesian model averaging with truncated normal components. *Comput Stat Data Anal*. 2014;75:227-238.
51. Carta JA, Ramírez P. Use of finite mixture distribution models in the analysis of wind energy in the Canarian Archipelago. *Energ Conver Manage*. 2007;48(1):281-291.
52. Mazzeo D, Oliveti G, Labonia E. Estimation of wind speed probability density function using a mixture of two truncated normal distributions. *Renew Energy*. 2018;115:1260-1280.
53. Higher Institute for Environmental Protection and Research (Istituto superiore per la protezione e la ricerca ambientale) ISPRA), Website: www.mareografico.it, last access: 28/05/2019.

54. National Renewable Energy Laboratory (NREL), National Wind Technology Center, NWTC M2 Tower, Website: www.nrel.gov, last access: 28/05/2019.

55. Curve Fitting Toolbox: for use with MATLAB®: User's Guide. Natick, MA: The MathWorks, Inc. 1994-2015. Website: https://it.mathworks.com/help/curvefit/index.html, last access: 28/05/2019.

How to cite this article: Mazzeo D, Oliveti G, Marsico A. A correction to the unimodal and bimodal truncated normal distributions for a more accurate representation of extreme and calm wind speeds. *Int J Energy Res*. 2019;1–34. https://doi.org/10.1002/er.4735

APPENDIX

MEAN, MEAN SQUARE, AND MEAN CUBIC WIND SPEEDS OF THE TND

$$V_{\mathrm{m1,TND}} = \frac{\int_0^{+\infty} v\left[\frac{1}{\sigma\sqrt{2\pi}}\exp\left[-\frac{1}{2}\left(\frac{v-\mu}{\sigma}\right)^2\right]\right]dv}{\int_0^{+\infty}\left[\frac{1}{\sigma\sqrt{2\pi}}\exp\left[-\frac{1}{2}\left(\frac{v-\mu}{\sigma}\right)^2\right]\right]dv} = \frac{\frac{\mu}{2}\left[1+\mathrm{erf}\left(\frac{\sqrt{2}\mu}{2\,\sigma}\right)\right]+\frac{\sigma}{\sqrt{2\pi}}\exp\left(-\frac{\mu^2}{2\sigma^2}\right)}{\frac{1}{2}\left[1+\mathrm{erf}\left(\frac{\sqrt{2}\mu}{2\,\sigma}\right)\right]} \tag{A1}$$

$$V^2_{\mathrm{m2,TND}} = \frac{\int_0^{\infty} v^2\left[\frac{1}{\sigma\sqrt{2\pi}}\exp\left[-\frac{1}{2}\left(\frac{v-\mu}{\sigma}\right)^2\right]\right]dv}{\int_0^{+\infty}\left[\frac{1}{\sigma\sqrt{2\pi}}\exp\left[-\frac{1}{2}\left(\frac{v-\mu}{\sigma}\right)^2\right]\right]dv} = \frac{\frac{1}{2}(\mu^2+\sigma^2)\left[1+\mathrm{erf}\left(\frac{\sqrt{2}\mu}{2\,\sigma}\right)\right]+\frac{\sigma\mu}{\sqrt{2\pi}}\exp\left(-\frac{\mu^2}{2\sigma^2}\right)}{\frac{1}{2}\left[1+\mathrm{erf}\left(\frac{\sqrt{2}\mu}{2\,\sigma}\right)\right]} \tag{A2}$$

$$V^3_{\mathrm{m3,TND}} = \frac{\int_0^{\infty} v^3\left[\frac{1}{\sigma\sqrt{2\pi}}\exp\left[-\frac{1}{2}\left(\frac{v-\mu}{\sigma}\right)^2\right]\right]dv}{\int_0^{+\infty}\left[\frac{1}{\sigma\sqrt{2\pi}}\exp\left[-\frac{1}{2}\left(\frac{v-\mu}{\sigma}\right)^2\right]\right]dv} = \frac{\frac{1}{2}\left[1+\mathrm{erf}\left(\frac{\sqrt{2}}{2}\left(\frac{\mu}{\sigma}\right)\right)\right](3\mu\sigma^2+\mu^3)+\frac{\sigma}{\sqrt{2\pi}}\exp\left(-\frac{\mu^2}{2\sigma^2}\right)(\mu^2+2\sigma^2)}{\frac{1}{2}\left[1+\mathrm{erf}\left(\frac{\sqrt{2}\mu}{2\,\sigma}\right)\right]} \tag{A3}$$